DOT/FAA/PS-89/4

Project Report
ATC-169

Use of Clutter Residue Editing Maps During the Denver 1988 Terminal Doppler Weather Radar (TDWR) Tests

D. P. Hynek

25 January 1990

Lincoln Laboratory
MASSACHUSETTS INSTITUTE OF TECHNOLOGY
LEXINGTON, MASSACHUSETTS

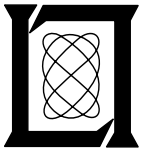

Prepared for the Federal Aviation Administration,
Washington, D.C. 20591

This document is available to the public through
the National Technical Information Service,
Springfield, VA 22161

TECHNICAL REPORT STANDARD TITLE PAGE

1. Report No.	2. Government Accession No.	3. Recipient's Catalog No.
ATC-169	DOT/FAA/PS-89/4	

4. Title and Subtitle

Use of Clutter Residue Editing Maps During the Denver 1988 Terminal Doppler Weather Radar (TDWR) Tests

5. Report Date
25 January 1990

6. Performing Organization Code

7. Author(s)
Daniel P. Hynek

8. Performing Organization Report No.
ATC-169

9. Performing Organization Name and Address
Lincoln Laboratory, MIT
P.O. Box 73
Lexington, MA 02173-9108

10. Work Unit No. (TRAIS)

11. Contract or Grant No.
DTFA-01-L-83-4-10579

12. Sponsoring Agency Name and Address
Department of Transportation
Federal Aviation Administration
Systems Research and Development Service
Washington, DC 20591

13. Type of Report and Period Covered
Project Report

14. Sponsoring Agency Code

15. Supplementary Notes

The work reported in this document was performed at Lincoln Laboratory, a center for research operated by Massachusetts Institute of Technology under Air Force Contract F19628-90-C-0002.

16. Abstract

The Lincoln Laboratory Terminal Doppler Weather Radar (TDWR) testbed operated in Denver, CO in 1987-88. This radar is a prototype of the wind shear detection radars scheduled to be installed by the FAA to provide warnings of possibly hazardous wind shear conditions in airport terminal areas. To obtain the required coverage at low altitudes (down to 100-200 meters above ground level), the antenna beam is required to scan at or very near the earth's surface. Strong ground clutter returns at these low elevation angles present a major problem in the detection of low reflectivity wind shear signals and pose a significant challenge to the mission of these radars.

To address this problem, steps along several fronts are taken to mitigate the effects of clutter contamination. These include the use of narrow pencil-beam antennas to minimize ground illumination, suppression by high-pass clutter filters, and the use of clutter residue map editing. This report deals with the latter step, and focuses on the clutter environment experienced at the testbed site during April-October 1988 and its effect on clutter residue map usage.

Since the clutter environment is subject to change over time — due either to man-made or natural causes — the residue maps require periodic updates to reflect the changing nature of the clutter. This is particularly important for radar systems such as these which rely on automated algorithms to detect subtle patterns and features in the radar returns. To study the frequency with which residue maps required replacement in Denver, clutter measurements recorded during this period were analyzed and are presented in this report as a series of clutter residue maps. The maps are compared and the short and long term changes analyzed. It is concluded that the overall changes during this time were relatively small and gradual, and that map updates at one to two month intervals were sufficient.

The generation of the residue maps is described and the importance of collecting clutter data on clear, weather-free days, without the presence of anomalous propagation conditions is addressed. This report also describes the use of median estimation in the construction of the maps as an effective method of eliminating the occasional strong returns from moving reflectors, such as aircraft and vehicles, which would otherwise distort the maps.

17. Key Words		18. Distribution Statement
clutter	pencil-beam	Document is available to the public through the National Technical Information Service, Springfield, VA 22161.
Doppler	weather radar	
hazardous		

19. Security Classif. (of this report)	20. Security Classif. (of this page)	21. No. of Pages	22. Price
Unclassified	Unclassified	76	

ABSTRACT

The Lincoln Laboratory Terminal Doppler Weather Radar (TDWR) testbed operated in Denver, CO in 1987-88. This radar is a prototype of the wind shear detection radars scheduled to be installed by the FAA to provide warnings of possibly hazardous wind shear conditions in airport terminal areas. To obtain the required coverage at low altitudes (down to 100 - 200 meters above ground level), the antenna beam is required to scan at or very near the earth's surface. Strong ground clutter returns at these low elevation angles present a major problem in the detection of low reflectivity wind shear signals and pose a significant challenge to the mission of these radars.

To address this problem, steps along several fronts are taken to mitigate the effects of clutter contamination. These include the use of narrow pencil-beam antennas to minimize ground illumination, suppression by high-pass clutter filters, and the use of clutter residue map editing. This report deals with the latter step, and focuses on the clutter environment experienced at the testbed site during April - October 1988 and its effect on clutter residue map usage.

Since the clutter environment is subject to change over time -- due either to man-made or natural causes -- the residue maps require periodic updates to reflect the changing nature of the clutter. This is particularly important for radar systems such as these which rely on automated algorithms to detect subtle patterns and features in the radar returns. To study the frequency with which residue maps required replacement in Denver, clutter measurements recorded during this period were analyzed and are presented in this report as a series of clutter residue maps. The maps are compared and the short and long term changes analyzed. It is concluded that the overall changes during this time were relatively small and gradual, and that map updates at one to two month intervals were sufficient.

The generation of the residue maps is described and the importance of collecting clutter data on clear, weather-free days, without the presence of anomalous propagation conditions is addressed. This report also describes the use of median estimation in the construction of the maps as an effective method of eliminating the occasional strong returns from moving reflectors, such as aircraft and vehicles, which would otherwise distort the maps.

TABLE OF CONTENTS

LIST OF ILLUSTRATIONS

LIST OF TABLES

LIST OF ACRONYMS

AGC	Automatic Gain Control
AP	Anomalous Propagation
ATC	Air Traffic Control
CPI	Coherent Processing Interval
FAA	Federal Aviation Administration
FIR	Finite Impulse Response (Filter)
FL-2	FAA/Lincoln Laboratory Testbed Doppler Radar
OT&E	Operational Test and Evaluation
PRF	Pulse Repetition Frequency
STC	Sensitivity Time Control
TDWR	Terminal Doppler Weather Radar

1.0 INTRODUCTION

The Terminal Doppler Weather Radar (TDWR) testbed, which operated in Denver, CO in 1987-1988, is a prototype of the planned TDWR system whose function is to detect and identify hazardous low altitude wind shear events at airports. This mission requires that the antenna beam be scanned very near to the earth's surface. The testbed operates at S-band and uses a 28-foot diameter antenna to generate a 1-deg pencil beam. (The operational TDWR system will operate at C-band with a pencil beam antenna pattern of 0.5 deg). Due to the local topography, an elevation angle of 0.3 degree was required in Denver which caused the lower portion of the antenna beam to illuminate much of the local terrain. Strong ground clutter returns at this low elevation angle presented a major challenge to detecting the often low cross-section signals from wind shear events.

To address the clutter problem, digital high-pass filters with narrow stopbands around zero Doppler velocity are employed to suppress near-stationary ground clutter. Extremely heavy fixed clutter and clutter from moving objects, however, are not fully suppressed by the filters and so additional measures are necessary. To suppress this remaining (residual) clutter, clutter residue maps are employed to edit the incoming data. These maps act as a spatial filter on the incoming data by establishing a threshold for each range-angle cell which determines whether a data point is valid or invalid. Operations in Denver during 1987-1988, which culminated in the Operational Test and Evaluation (OT&E) demonstration in July and August 1988, used clutter residue maps [1] for clutter editing as one of several advanced processing techniques.*

---

* Other advanced processing techniques employed during this time included the use of new digital clutter filters [2], automatic PRF selection to minimize obscuration due to out-of-trip clutter returns [3], and automated wind shear detection algorithms [4].

In support of the clutter map development, carefully controlled radar clutter measurements were made periodically through the 1988 spring-to-fall period from which the clutter maps were subsequently generated. One uncertainty related to the operational use of these maps was the period of time for which a particular map remained valid. With expected seasonal changes in vegetation and possibly man-made structures, there would be a need for periodic map updates to accurately reflect the new clutter conditions. It was expected that the maps would be useful over some unknown short term (days and possibly weeks at a time), but that longer term changes would alter the basic structure of the clutter and would require new maps. To address this uncertainty, the maps generated during this time were compared and an attempt made to characterize the changes and to estimate their useful life. Selected maps are presented in this report, along with difference maps (where one map is subtracted from another) which highlight the clutter residue changes taking place over different time intervals.

2.0 THE CLUTTER PROBLEM

Figure 1 illustrates the relative locations of the radar, the airport, the city, and the mountains in the Denver area as viewed on a radar PPI scan.

Figure 2 shows radar clutter maps covering the northwest sector from the radar site that encompasses Stapleton International Airport. These maps were made at an elevation angle of 0.3 deg. (During the Denver operations, clutter residue maps were used at 0.3, 0.5, and 1.0 deg elevation). Figure 2(a) was recorded without clutter filters, and Figure 2(b) is the corresponding map recorded with a 1 m/s stopband filter. The unfiltered map shows very intense clutter over most of the region, the most prominent features being the Rocky Mountains about 45 km away. There is also considerable clutter at closer ranges from the Denver metropolitan area.

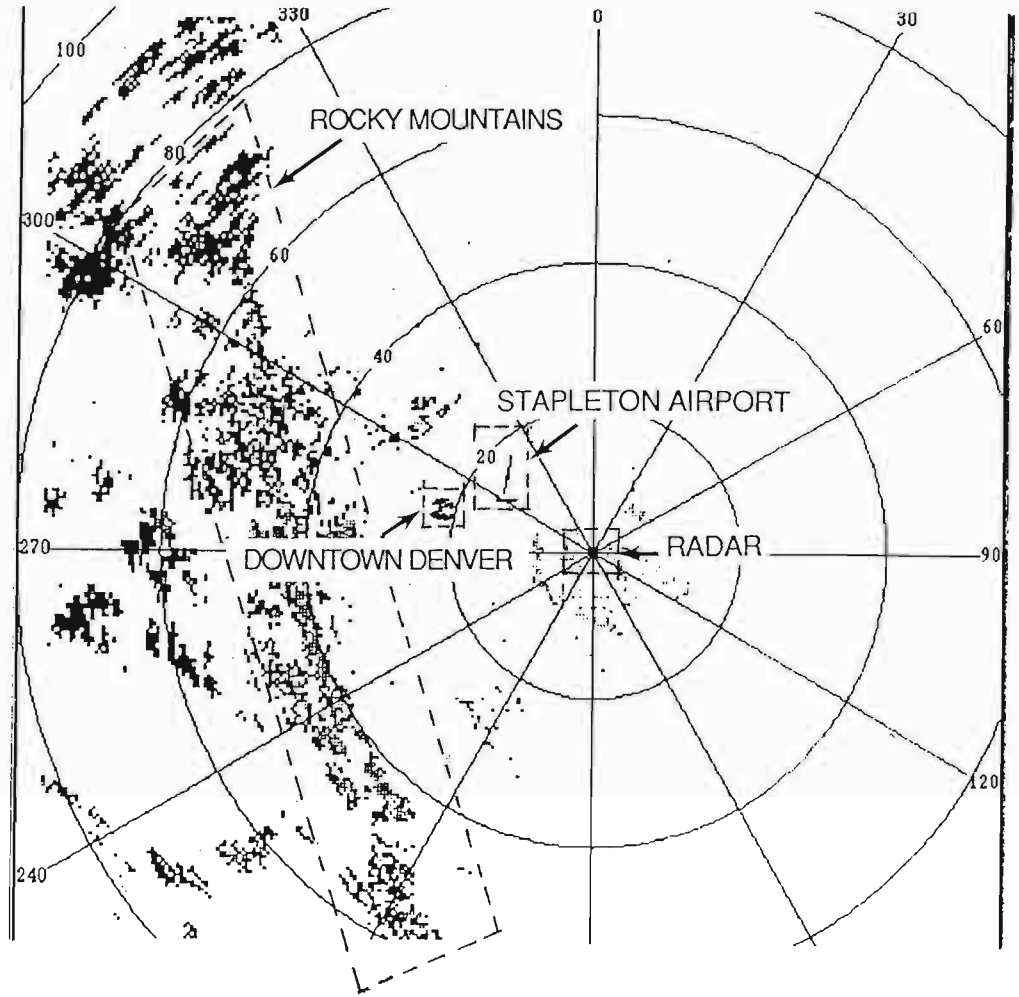

Fig 1. Relative locations of radar site, Stapleton airport, and other features in Denver area.

Figures 2(c) and 2(d) show an enlarged view of the same maps, magnifying the airport vicinity (the runway locations are overlayed on these maps). The filtered maps show that a great deal of clutter has been removed, both in the mountain region and particularly in the immediate vicinity of the airport, which was the primary region of coverage. Although much of the near-stationary clutter has been suppressed,* a significant amount of residual clutter still remains which must be mitigated by the residue editing step.

The editing process compares the incoming signal with the corresponding residue map range-angle cell, and declares it valid if it exceeds the map value, and invalid if it does not. In this way, particular cells consisting primarily of clutter returns are flagged so as not to corrupt the weather detection algorithms with bad data which could, for example, occur in the middle of a wind shear event and cause it to be missed, or cause excessive false alarms.

An example of clutter residue editing applied to actual weather data appears in Figure 3. Plate (a) shows a 360-deg weather scan recorded on July 8, 1988. A storm was moving through the area from the southwest to the northeast. Large storm cells are visible directly to the south. Some storm cells are moving over the mountain region to the west, but are difficult to discern on this intensity plot because of strong clutter returns from this region. Plate (b) shows the same data after clutter residue editing. One prominent storm cell at about 280 deg azimuth and 50 km range (circled on the maps) is visible to the eye at this point. In the velocity field (not shown), the stationary velocity returns from the mountains, which could be

---

* The active clutter filters are designed to give 50 dB of attenuation at the band center; this has been demonstrated on fixed targets with the antenna stationary. Under operational conditions, with the antenna rotating at 25 deg/s, clutter suppression in Denver ranged from 35 dB to 50 dB depending on the composition of the clutter.

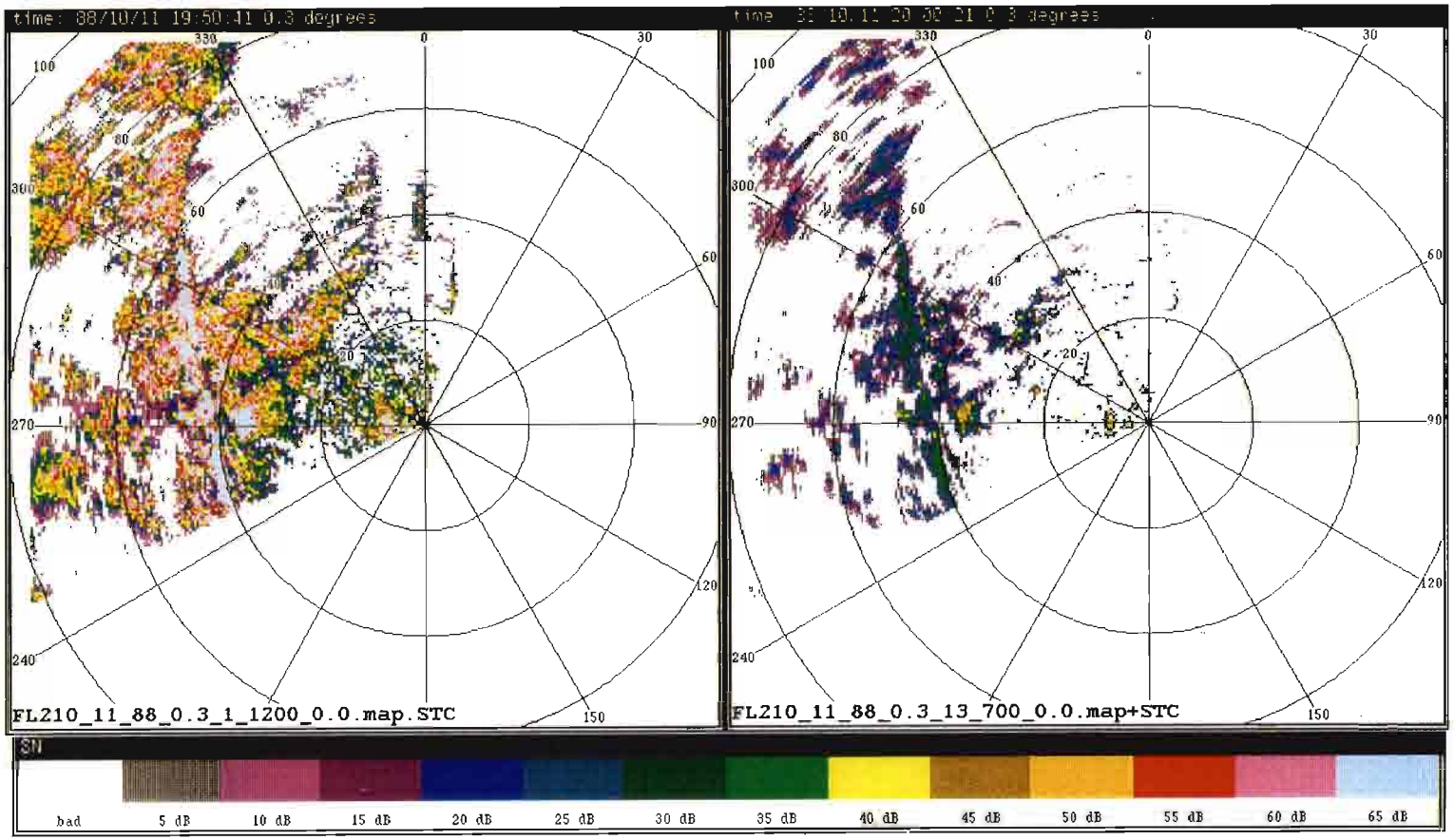

(a) (b)

Fig 2. Denver area ground clutter maps. (a) Without clutter filter, (b) With 1 m/s stopband clutter filter, (c) Enlarged view of (a), (d) Enlarged view of (b).

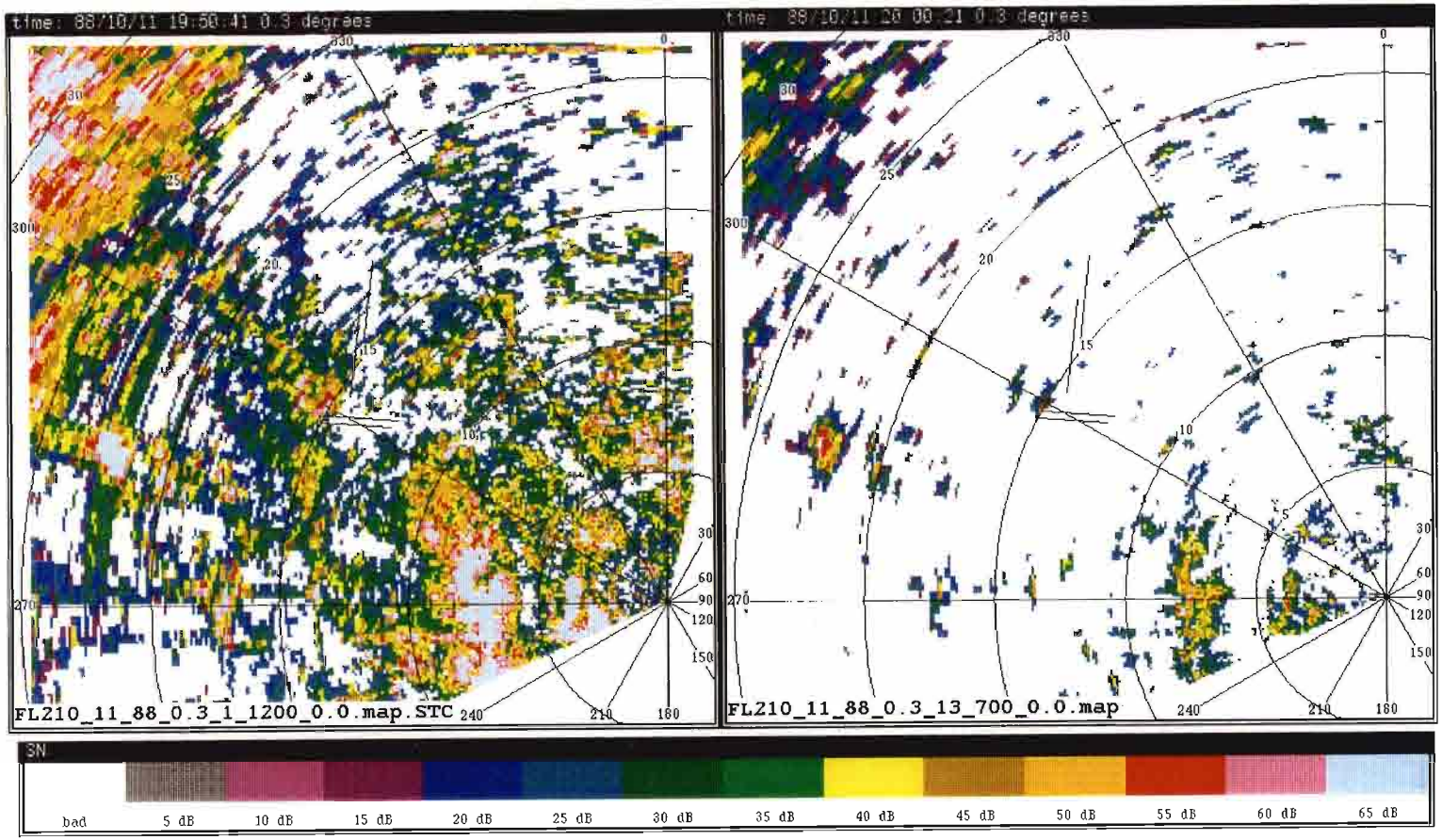

(c) (d)

Fig 2. (continued) Denver area ground clutter maps. (a) Without clutter filter, (b) With 1 m/s stop-band clutter filter, (c) Enlarged view of (a), (d) Enlarged view of (b).

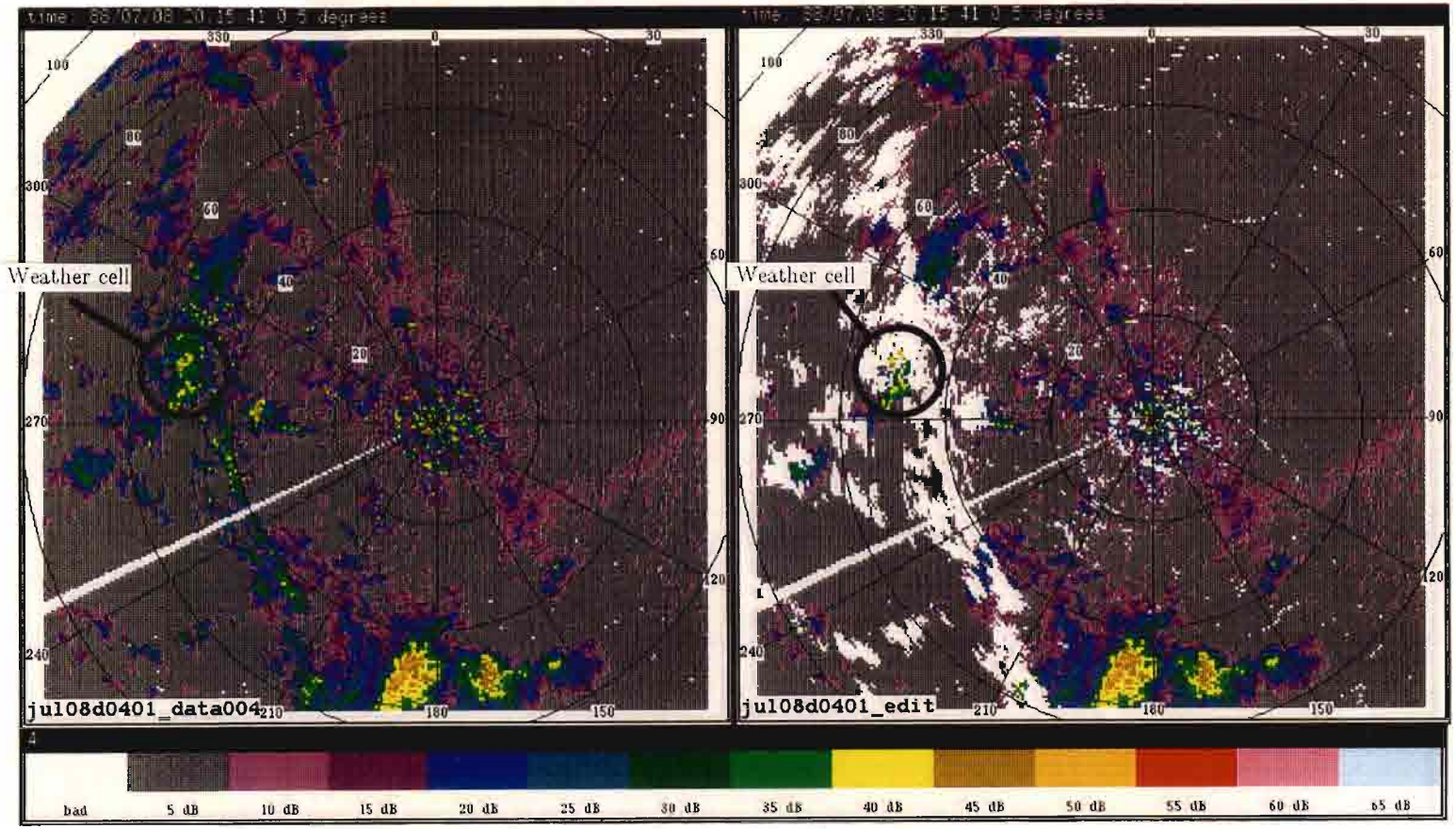

(a) (b)

Fig 3. Example of clutter residue editing. (a) Scan of weather data without editing, (b) Same data with clutter residue editing.

interpreted falsely by the automatic algorithms as being a component of convergence or divergence in an otherwise uniform wind field, are effectively removed by being declared invalid.

Clutter residue editing has had a particular impact on the reliability of gust front algorithm performance. During the 1987 summer experimental season before the clutter maps were placed into use, a detection false alarm rate of about 44% was experienced. After implementation of the maps, the false alarm rate dropped to about 2.4% [5]. Clearly, effective ground clutter rejection is essential to reliable performance of this algorithm. The automated microburst detection algorithm is also potentially sensitive to the clutter field. Its performance relative to different map variables is being evaluated.

Clutter residue editing also provides improved quality for the precipitation product used by Air Traffic Control (ATC) supervisors for planning purposes. In Figure 2(c), for example, the clutter residue could be mistakenly interpreted by ATC as a set of thunderstorms. Another problem with clutter residue is that it can appear to be precipitation and cause the operational TDWR, which is an automated system, to switch from monitoring mode to the hazardous weather mode. Editing thus plays a significant role in largely eliminating strong clutter regions and consequently increasing the overall credibility of the TDWR system.

3.0 CLUTTER RESIDUE MAP GENERATION

3.1 Map-Making Procedure

A typical map is created from about 20 consecutive clutter measurement scans at a particular elevation angle. The median value of the 20 scans is taken as the estimate of ground clutter residue intensity at each range-azimuth cell of the map (an original version of the maps used the arithmetic mean of the 20 scans).

Measurements are made on clear, weather-free days, without the presence of anomalous propagation conditions.

"Clear-air" returns, often measurable on these days and due to various low reflectivity wind-blown tracers in the air or refractive index irregularities, should not appear in the clutter residue editing map as these returns can provide information on low reflectivity wind shear events. Consequently, range-azimuth cells whose apparent clutter residue level is less than or equal to the expected clear-air returns are assigned a value which results in no clutter residue editing. The clear-air reflectivity estimate is established by measurements near the surface which do not have clutter, and which have velocities above a site-dependent threshold.

Provision is made to manually edit and override map values in order to alter certain map features, as necessary. The residue associated with moving vehicles on highways or other spurious non-stationary targets, for example, are removed in this manner. Also, certain cells can be flagged where strong echoes saturate the receiver, such as those received from certain close range targets and, in the Denver case, the returns from the downtown buildings. With this editor, called the "polygon" editor, one can specify the corners of an arbitrary polygon which encloses the map area to be assigned a specified value.

When the map is fully processed, a final operational adjustment is made before the map is used for editing. All map values are scaled by a value Xcr, a site-adaptable parameter, which uniformly adjusts all map values upward (typically by 5 to 10 dB). The Xcr value is selected to minimize the amount of clutter breakthrough due to short term fluctuations of the clutter returns. Since the raw map values are the calculated median of a large number of clutter scans, many individual measurements exceed the map value and consequently "break through".

The Xcr value is empirically established to minimize this breakthrough without over-editing legitimate weather returns. The optimum value of Xcr is that value which optimizes the detection and false alarm probabilities of the automatic wind-shear algorithms for the particular clutter conditions present [1].

3.2 Median Versus Average Maps

The first maps created during the 1988 season were generated by time-averaging 20 clutter scans per elevation angle. Part way through the season, it was found that these maps produced results that were inconsistent with expected performance. Particularly troublesome was the presence of aircraft returns along the approach and departure routes at Stapleton and other airports in the Denver area. Although many of these spurious targets were edited with the polygon editor, particularly those recognizable because of their predictable flight patterns, other such targets nevertheless escaped scrutiny and remained in the map. Furthermore, the use of the polygon editor tended to be a "broad-brush" approach to the problem in that legitimate ground clutter returns that should have remained in the map were also edited because of their proximity to offending targets. After this experience with the first operational maps, it was decided to make a fundamental change in the map-making technique from one of simple temporal averaging, to one using the temporal median of the data points in each range-azimuth cell. This was done with the expectation that the sporadic large returns from aircraft could be reduced or largely eliminated in the final map, by being treated as outliers and given less statistical weight in the computation of a cell's value.

Figures 4(a) and 4(b) illustrate the difference between the two processing schemes. Both maps were generated from the same 20 scans of clutter data. Plate (a) is representative of the early maps that used cell averaging. Plate (b) was

generated using the median value of the 20 measurements. The differences between the two maps are immediately obvious and striking. The large number of aircraft returns at the north end of the north-south runways and at the east end of the east-west runways are largely eliminated. The cluster of returns to the north at about 352 deg and 20 km, believed to be a flock of large water fowl, has also been mostly removed (a "yellow-level" target remaining may not be reproducible). Also, one can notice the significant reduction in echoes from moving vehicles along Interstate I-70, due north at a range of 5 to 7 km. Moreover, strong stationary clutter features show little or no change, as for example, the downtown Denver buildings (azimuth 285 deg, range 22 km) which are nearly identical, pixel for pixel in the two maps. Figures 4(c) and 4(d) are the corresponding full-range maps of the Denver area. These maps show a general elimination of the random, isolated returns visible over most of the area in the averaged maps.

Figure 5 shows plots of the data points that went into two particular cells containing aircraft returns at the end of the runways. The 20 data values, one measured for each scan, are plotted along the horizontal axis. Figure 5(a) is a case where only one large return was recorded (62 dB SNR on scan 15), with the other 19 points reading 0 dB or less. In the averaging case (power averaging is used, not log averaging), this one return dominates the result for that cell, which has an average value of 49 dB and consequently shows up as a strong map feature. The median computation, on the other hand, results in a value of less than 0 dB, and this return is suppressed in the map. Figure 5(b) shows the 20 data points in a second cell containing an aircraft return in the same vicinity. In this case, there are several more hits which contribute to a high average value. Here again, with the majority of the data points and hence the median value near 0 dB, these returns are suppressed in

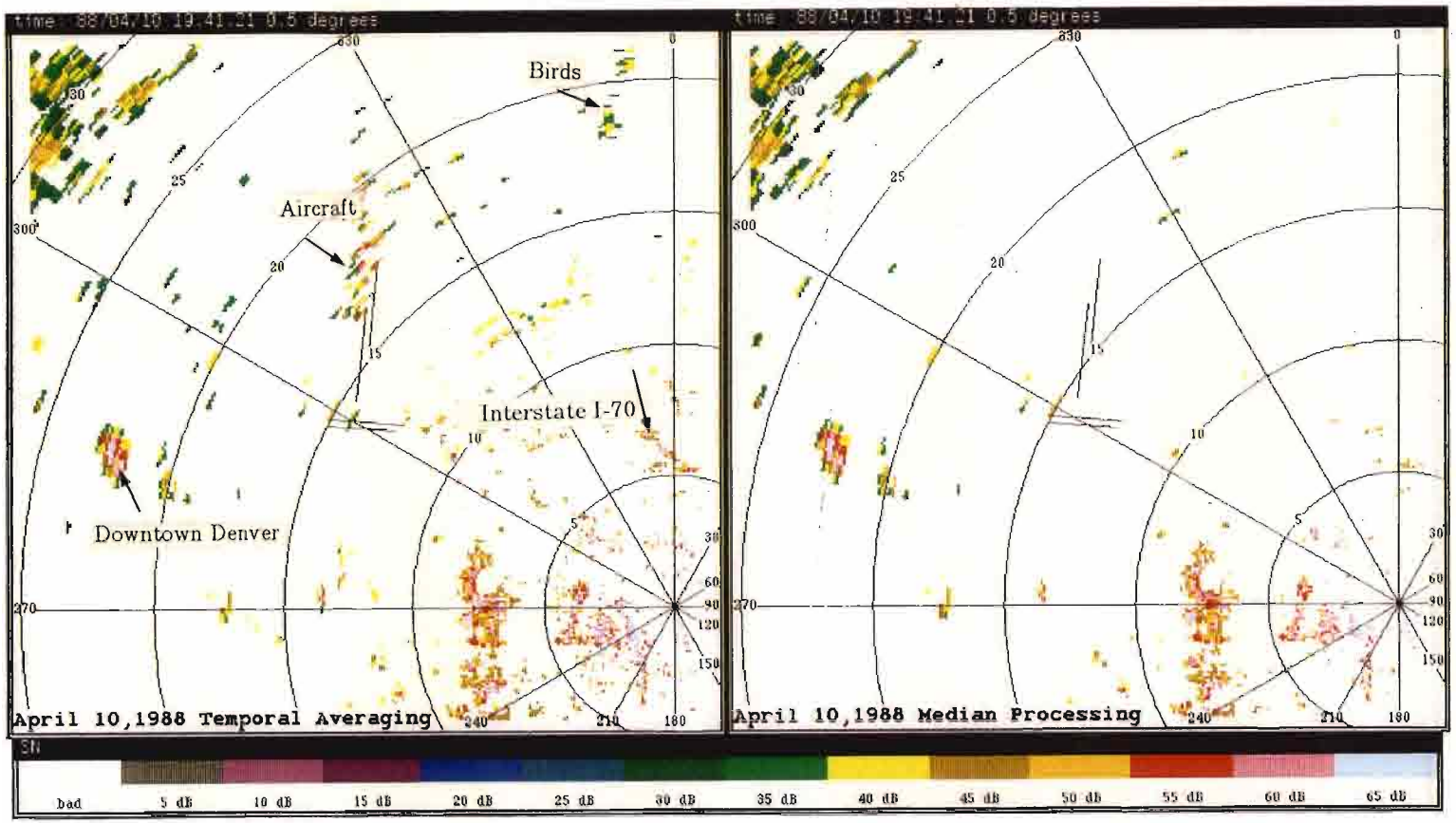

(a) (b)

Fig 4. Comparison of clutter residue maps generated by *averaging* or taking *median* value of clutter measurements. (a) Average value of 20 scans, (b) Median value of 20 scans, (c) Full-range view of (a), (d) Full-range view of (b).

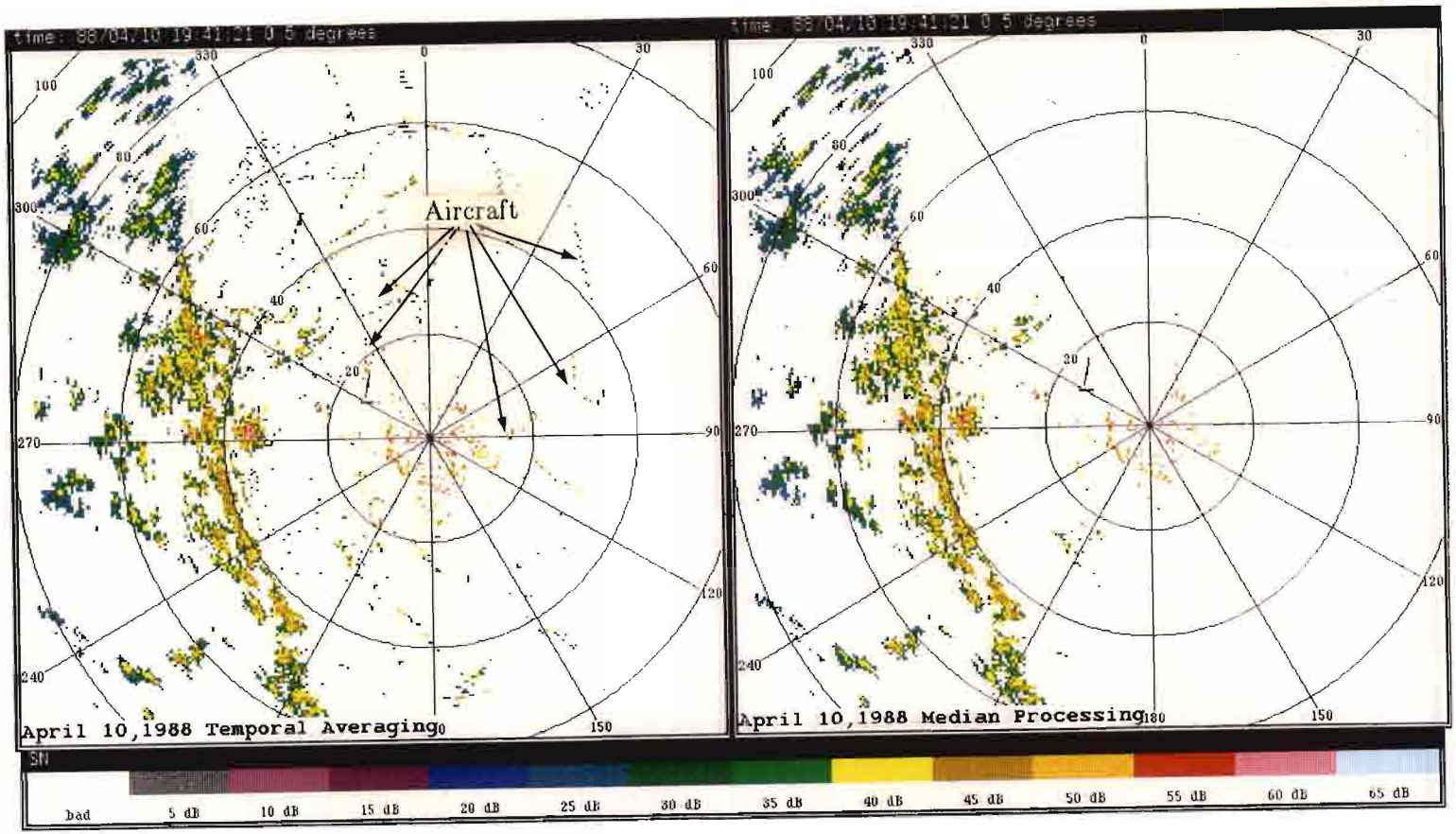

(c) (d)

Fig 4. (continued). Comparison of clutter residue maps generated by *averaging* or taking *median* value of clutter measurements. (a) Average value of 20 scans, (b) Median value of 20 scans, (c) Full-range view of (a), (d) Full-range view of (b).

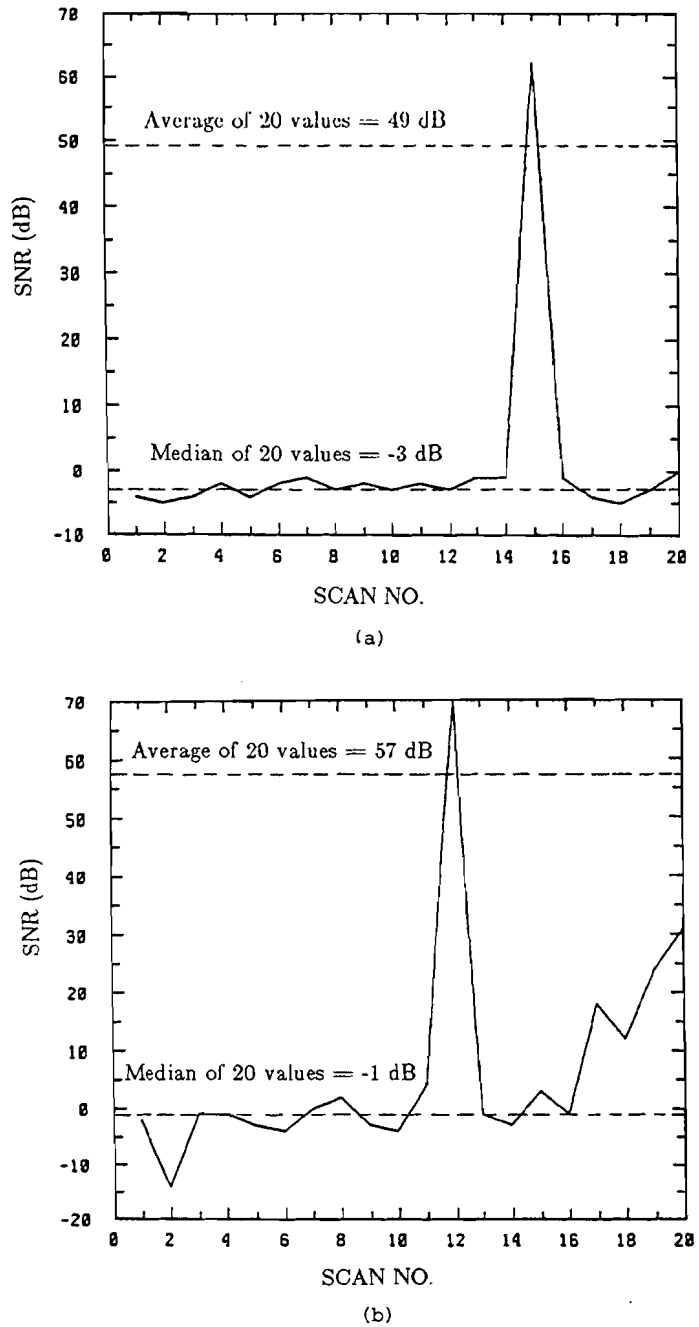

Fig 5. Data points recorded for 20 consecutive clutter measurements (one per scan) at two range-angle cells containing aircraft returns. (a) Range = 17.24 km, azimuth = 318.5 deg, (b) Range = 17.96 km, azimuth = 318.5 deg.

the median version of the map.

The median maps were placed into operational use in Denver in mid-August 1988. With the successful removal of most of the unwanted features, the time-consuming process of manually identifying and editing these artifacts was greatly reduced. Along with the new map software, a provision was added to automatically identify and flag saturated cells, further minimizing the need for manual intervention in the map-making process. Thus, the changeover to median processing resulted in a significant improvement in the quality of the maps and in the effort required to generate them.

4.0 INSTRUMENTATION CONSIDERATIONS

4.1 Radar Characterisics

The technical parameters of the TDWR testbed radar are listed in Appendix A. Certain radar characteristics pertinent to its weather and clutter measurement role are briefly described here.

Weather parameter estimation is done by pulse-pair processing. The three primary parameters: reflectivity, mean velocity and spectrum width, are computed from the 0th, 1st, and 2nd moments, respectively.

The radar operates in an indexed-beam mode, whereby data are always recorded on the same angle boundary (every 1 deg, which corresponds to the nominal antenna half-power beamwidth). This means that the number of radar pulses integrated in each resolution cell is variable (since *all* the pulses received during that 1 deg interval are integrated), and is a function of the instantaneous antenna scan rate and the PRF. (This is called the coherent processing interval, or CPI, and is measured in terms of the number of pulses integrated). The angle-indexing feature simplifies the map generation process in that fewer measurement scans are needed to obtain a

fixed number of samples in each resolution cell for statistical stability.* This significantly minimizes the time required to record the clutter data and to generate the maps.

The radar range measurement is recorded in 800 gates with a basic range resolution of 120 m. Thus, the radar records all data in resolution cells that are 1 deg by 120 m in size.

4.2 Clutter Filters

The clutter filters are digital high-pass FIR (Finite Impulse Response) filters that suppress signal returns near zero Doppler velocity. Their idealized frequency response is shown in Figure 6(a). A choice of three filters is available at any given PRF, corresponding to stopband widths of 1/3, 2/3, and 1 m/s. This set of filter widths is available in each of four different PRF bands, as listed in Figure 6(b). Attenuation near zero velocity is nominally 50 dB for each of the filters. This amount of clutter suppresion is realized only for an antenna that is stationary or moving at a very slow rate. In an operational case, with an antenna scan rate of about 25 deg/s (as is the case for clutter measurements), scan modulation produces spectral broadening of the clutter returns (spectral broadening due to antenna motion is proportional to antenna scan rate). This, combined with receiver errors** and/or clutter source movement, can reduce the effective clutter suppression to as low as 35 dB.

---

* Non-indexed beam processing requires finer angular resolution maps (on the order of 0.1 to 0.25 deg for a 1-deg beamwidth) and thus requires a many-fold increase in the number of clutter scans to ensure a large enough number of measurements in each range-azimuth cell.

** 1989 testing in Kansas City, MO found that errors in AGC normalization were causing "steps" in the data supplied to the clutter filters. These steps had substantial energy in the clutter filter passband and hence reduced the effective clutter suppression. This problem may have existed in the Denver testing in 1988 and caused the effective suppression to be about 35 dB.

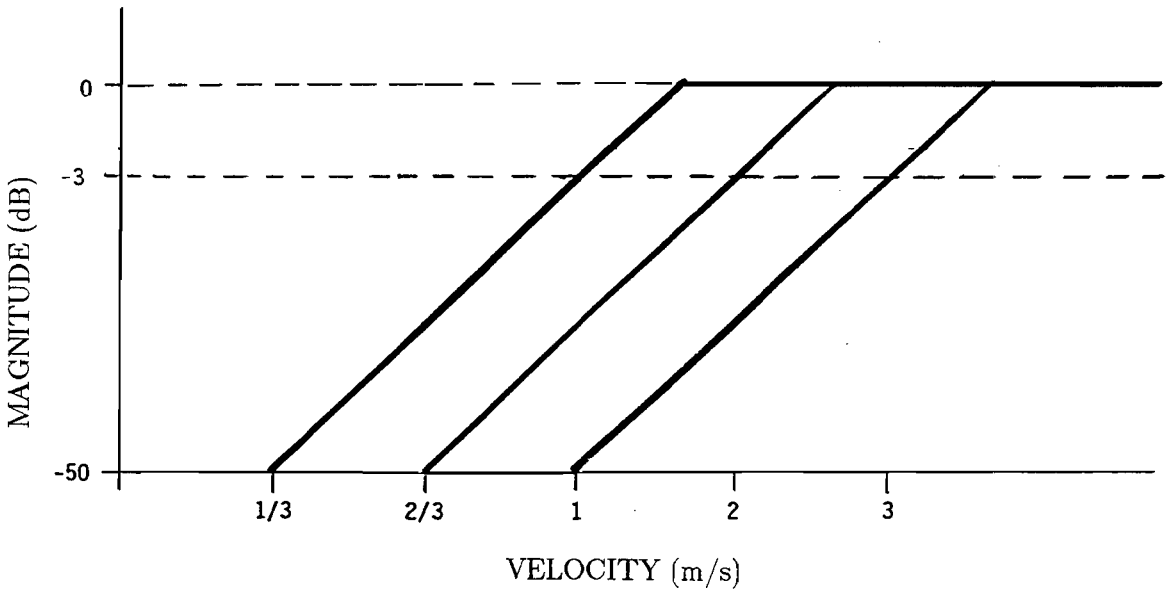

(a)

Filter Set	Stopband Edge (m/s)	Passband Edge (m/s)	Design PRF (pps)	PRF Range (pps)
1	All Pass	---	----	700-1220
2	1/3	1	1200	1126-1220
3	2/3	2		
4	1	3		
5	1/3	1	1050	976-1125
6	2/3	2		
7	1	3		
8	1/3	1	900	801-975
9	2/3	2		
10	1	3		
11	1/3	1	700	700-800
12	2/3	2		
13	1	3		

(b)

Fig 6. Clutter filter characteristics. (a) Idealized filter frequency response, (b) Operational filter parameters.

All clutter measurements were recorded with the widest operational filter (1 m/s stopband) at the lowest PRF allowable in each PRF band. This is the "worst-case" operation for each filter (provides least clutter suppression), since the filter design is such that the bandwidth is proportional to PRF, and thus the low end of the band represents the narrowest realization of that filter. In actual operation, the PRFs are determined by independent criteria (such as minimum obscuration rules) and the appropriate filters are inserted for the chosen PRF.

The choice of filter widths is usually a compromise between the need to suppress near-stationary ground clutter and the desire to retain low velocity wind shear features with minimum suppression.

4.3 Sensitivity Time Control (STC)

The use of STC became operational part way through the 1988 season. This feature inserts attenuation in the receiver front-end -- inversely with range -- for the first 10 km to suppress close-in clutter targets that might otherwise saturate the receiver, and to provide a constant receiver sensitivity (in reflectivity factor, Z, terms) at close ranges. A maximum attenuation of 40 dB is inserted at zero range, followed by a 1/range-squared law falloff to zero dB at 10 km range (full receiver gain is restored at a range of 10.08 km). This produces a constant reflectivity sensitivity of about -20 dBz over this range interval. STC makes possible the observation of strong, close range weather events that might otherwise saturate the receiver. It effectively shifts the available receiver dynamic range upward to handle the stronger signals. A correction is applied to the recorded reflectivity value to account for this added attenuation.

The earliest clutter residue maps were recorded without STC. Subsequent maps were recorded with STC to match the operating mode of the radar. Both types of

maps are presented in this report.

5.0 AVAILABLE CLUTTER DATA

Table 1 lists the clutter data gathered for the three principal elevation tilts during the 1988 experiment. The 0.3, 0.5, and 1.0 deg tilts conform to the elevation scan strategy employed for the microburst and gust front algorithms during this time. At each elevation angle, data were recorded with four different clutter filters, one for each of the PRF bands listed. STC was activated starting with the July 9 clutter runs. The maps chosen for presentation in this report (to be described subsequently in Figures 7 through 11) were selected from the set recorded at 0.3 deg elevation and a PRF of 700 pps, using a clutter filter with a stopband width of 1 m/s.

6.0 DENVER CLUTTER RESIDUE MAPS

Figures 7 through 11 are actual clutter residue maps generated for the April through October 1988 time-frame as indicated in Table 2. These maps were constructed using median processing and are shown before clear-air thresholding. They are Cartesian coordinate versions of the maps that operationally exist in polar coordinate form. The resampling and transformation to Cartesian coordinates is done to simplify the display and interpretation of radar weather data. In this form the data can be viewed in constant-sized Cartesian cells rather than the PPI format in which the data are naturally collected. Plate (a) of each figure displays a full-scale view of the map out to a range of 92 km (resampled to 500 m Cartesian cells); plate (b) of each figure enlarges the area around Stapleton Airport (resampled to 100 m cells). The first two maps (April 10 and May 12) have 360-deg coverage around the radar site; subsequent maps cover a 120-deg sector centered on the airport.

TABLE 1

DENVER 1988 CLUTTER DATA AVAILABLE FOR RESIDUE MAPS FOR 0.3,0.5,1.0 DEG. TILTS

ELEV	APR 10		MAY 12		JUN 21 (test)		JUL 9		JUL 10		JUL 21		AUG 13		AUG 24		OCT 11		OCT 22		PRF
	STC		STC		STC		STC		STC		STC		STC		STC		STC		STC		
	ON	OFF	ON	OFF	ON	OFF	ON	OFF	ON	OFF	ON	OFF	ON	OFF	ON	OFF	ON	OFF	ON	OFF	
0.3		X		X		X	X		X						X	X	X		X	X	1126
		X		X		X	X		X						X	X	X		X	X	976
		X		X		X	X		X						X	X	X		X	X	801
		X		X		X	X		X						X	X	X		X	X	700
0.5		X		X		X				X			X		X	X	X		X	X	1126
		X		X		X				X			X		X	X	X		X	X	976
		X		X		X				X			X		X	X	X		X	X	801
		X		X		X				X			X		X	X	X		X	X	700
1.0		X		X		X				X	X						X		X	X	1126
		X		X		X				X	X						X		X	X	976
		X		X		X				X	X						X		X	X	801
		X		X		X				X	X						X		X	X	700

TABLE 2

CLUTTER RESIDUE MAPS FOR APRIL TO OCTOBER 1988

(All 0.3 deg elevation angle)

Figure	Date	STC Status
7a,b	April 10	Off
8a,b	May 12	Off
9a,b	July 9	On
10a,b	August 24 (anomalous)	On
11a,b	October 11	On

6.1 Fixed Clutter Features

The mountains to the west and northwest are the most prominent fixed features in Figures 7 through 11. The region to the east and south, representing the plains east of Denver, has relatively little residual clutter. Dominant man-made features clearly stand out in the enlarged maps; notably, the buildings at the west end of the east-west runways and the downtown Denver buildings (azimuth 285 deg, range 22 km), which exhibit strong enough returns to saturate the receiver and which are also visible in the far-out antenna sidelobes. The faint pair of concentric arcs at azimuths 0 to 45 deg and 165 to 215 deg, range 22 km (best seen in Figures 7(a) and 8(a)) are manifestations of the Denver buildings in the far-out sidelobes. These odd features were first noted by Rinehart [6], who pointed out that they had velocities associated with them that were a function of scanning direction and speed, and are caused by the motion of the feedhorn as the antenna rotates in azimuth. At about azimuth 270 deg, range 35 km, large returns are also visible from the build-

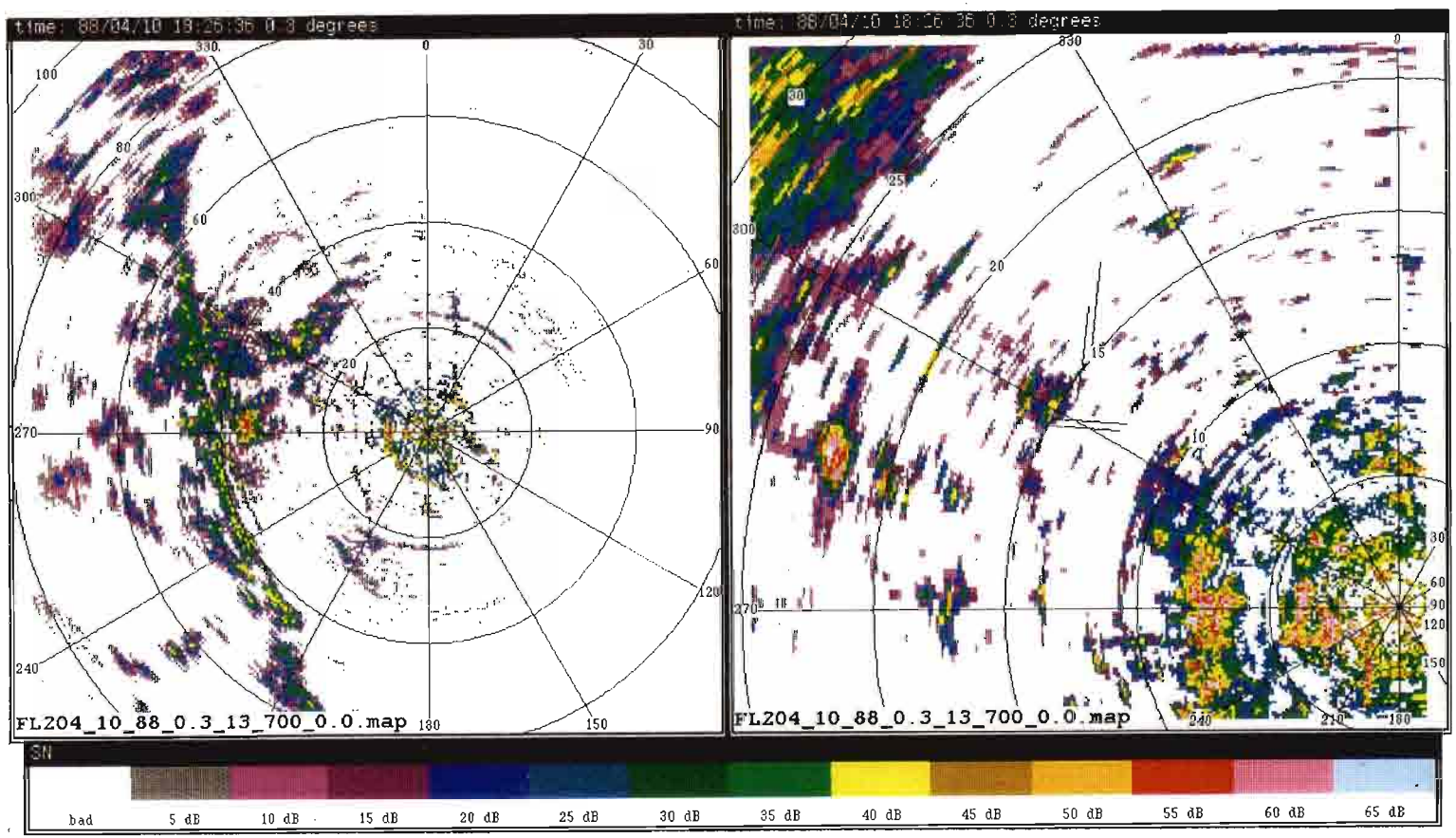

(a) (b)

Fig 7. Clutter residue map for April 10, 1988, STC off. (a) Full range view, (b) Enlarged view of Stapleton airport area.

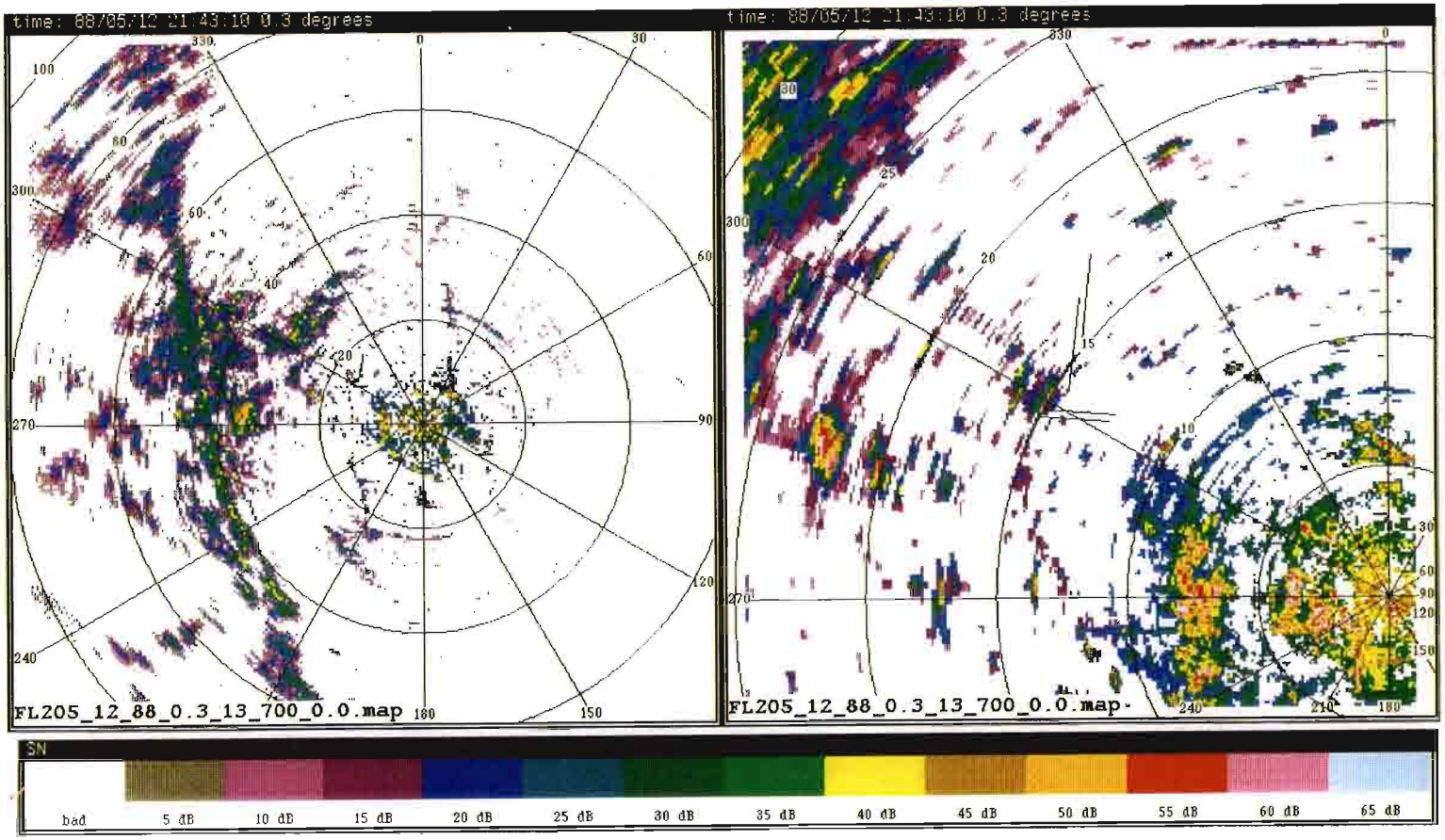

(a) (b)

Fig 8. Clutter residue map for May 12, 1988, STC off. (a) Full range view, (b) Enlarged view of Stapleton airport area.

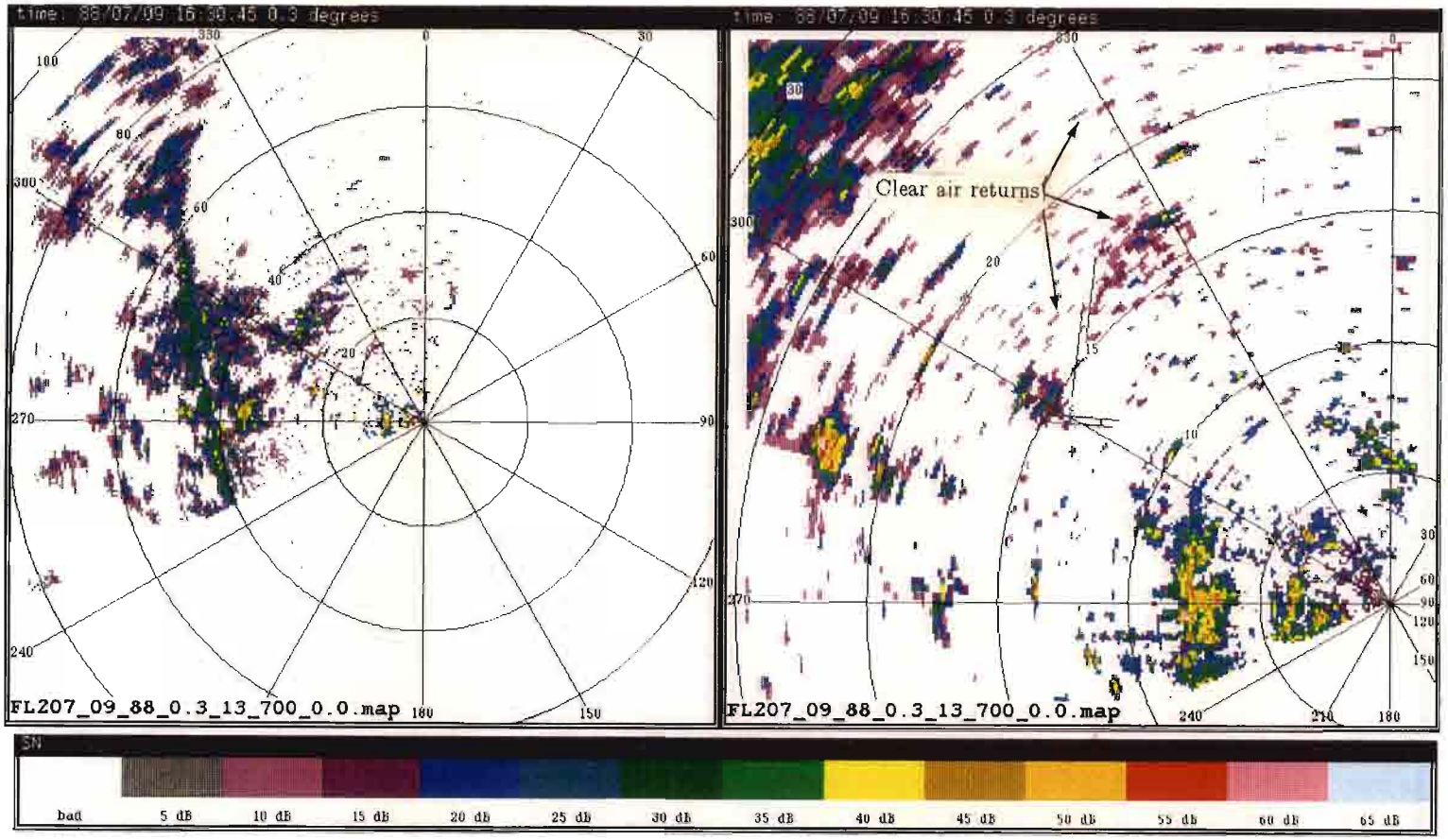

(a) (b)

Fig 9. Clutter residue map for July 9, 1988, STC on. (a) Full range view, (b) Enlarged view of Stapleton airport area.

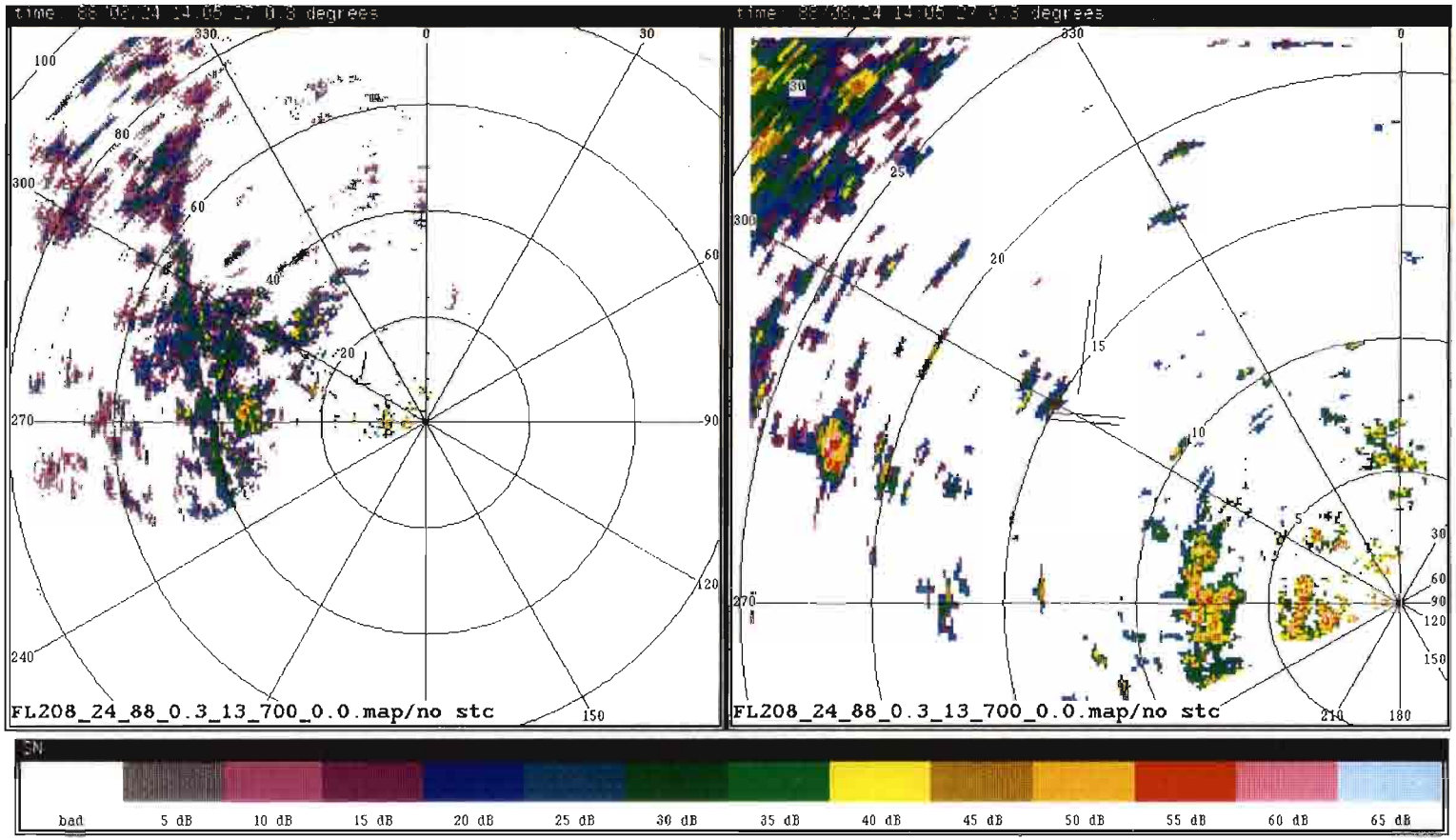

(a) (b)

Fig 10. Clutter residue map for August 24, 1988, STC on. (a) Full range view, (b) Enlarged view of Stapleton airport area.

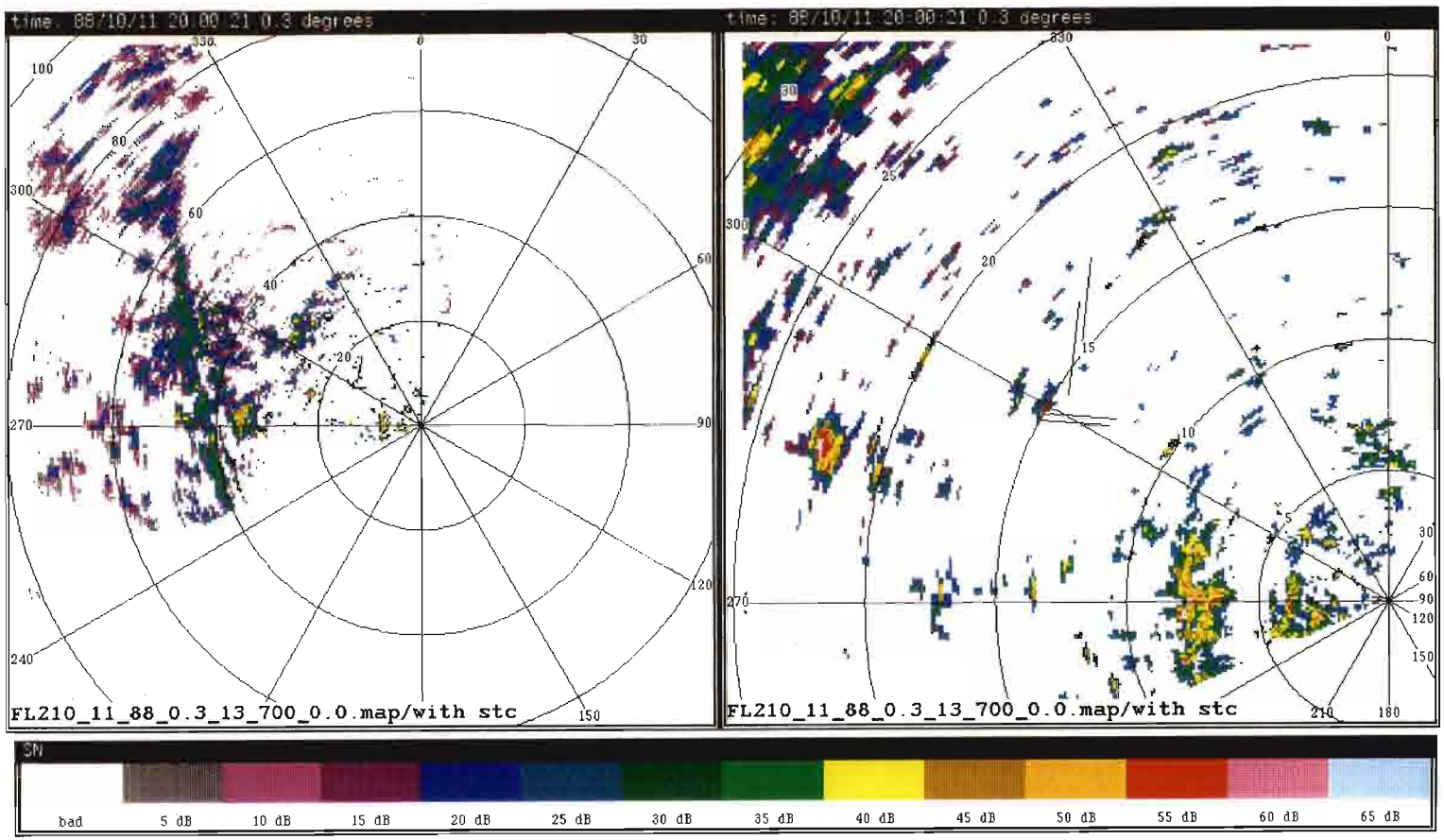

(a) (b)

Fig 11. Clutter residue map for October 11, 1988, STC on. (a) Full range view, (b) Enlarged view of Stapleton airport area.

ing complex in the vicinity of the Denver Federal Center.

Evident also on some of these maps (annotated in Figure 9) are clear-air returns -- the weak signals randomly scattered around the maps. These features are shown here for illustration purposes but are removed in the actual operational maps by thresholding at the level of the clear-air return estimate.

6.2 Clutter Residue Changes

To highlight the changing nature of the clutter residue over time, the various maps were compared and are presented in this section as difference maps, where one map is subtracted from another, and the difference is presented in the same map format. First, to show residue changes over increasingly longer periods of time, the difference is taken between each map and the first map in the set (April 10). Following this, comparisons are made on a map-to-map basis to show changes over shorter periods of time.

6.2.1 Baseline Case

As a baseline case, the difference between two maps generated about 2.5 minutes apart is taken as a practical measure of the short term variability to be expected between maps. The global statistics are also computed for each of the difference maps (mean and standard deviation for the entire map).*

Figure 12 is the difference map for the short term (2.5 minute) baseline case. Wind speed was about 6 knots from 280 deg when these clutter measurements were made. Visually, this comparison shows that the maps are very similar, as indicated by the fairly small peak fluctuations of 4 to 6 dB and a small mean difference. The

* Since some of the maps have STC applied and others do not, the first 10 km of range are not included in the statistics if there is a disparity in STC status between the two maps being compared.

computed statistics for the entire map indicate a mean difference value of -0.2 dB with a standard deviation of 2 dB. This result represents the visual and statistical difference to be expected between two clutter field estimates made over the short term. Scan-to-scan clutter distributions were not available; however, for comparison purposes, measurements made with an ASR testbed at S-band in Huntsville, AL in April 1987 by Weber [7] indicated peak clutter fluctuations of about 7 dB about the average of a 100 scan set of clutter measurements over a variety of terrain features.

6.2.2 Extended Term (Seasonal) Clutter Residue Changes

Figure 13 shows a sequence of difference maps relative to April 10. Plate (a) is the actual clutter residue map for April 10; plates (b), (c) and (d) portray the clutter difference for progressively longer periods of time referenced to April 10. Plates (e) through (h) are the corresponding enlarged maps of the airport area. The time intervals between these maps range from 32 to 184 days, as indicated in Table 3. Also listed are the overall statistics computed for each difference map.

TABLE 3

DIFFERENCE MAPS REFERENCED TO APRIL 10,1988

Figure	Dates	Time Span	Difference Statistics	
			Mean	Std Dev
12a,b	Oct 22 - Oct 22 (baseline ref)	2m 25s	-0.2dB	2.0dB
13b,f	Apr 10 - May 12	32 days	1.1	3.7
13c,g	Apr 10 - Jul 9	90	3.5	4.3
----	Apr 10 - Aug 24 (anomalous)	136	2.8	6.2
13d,h	Apr 10 - Oct 11	184	4.1	4.3

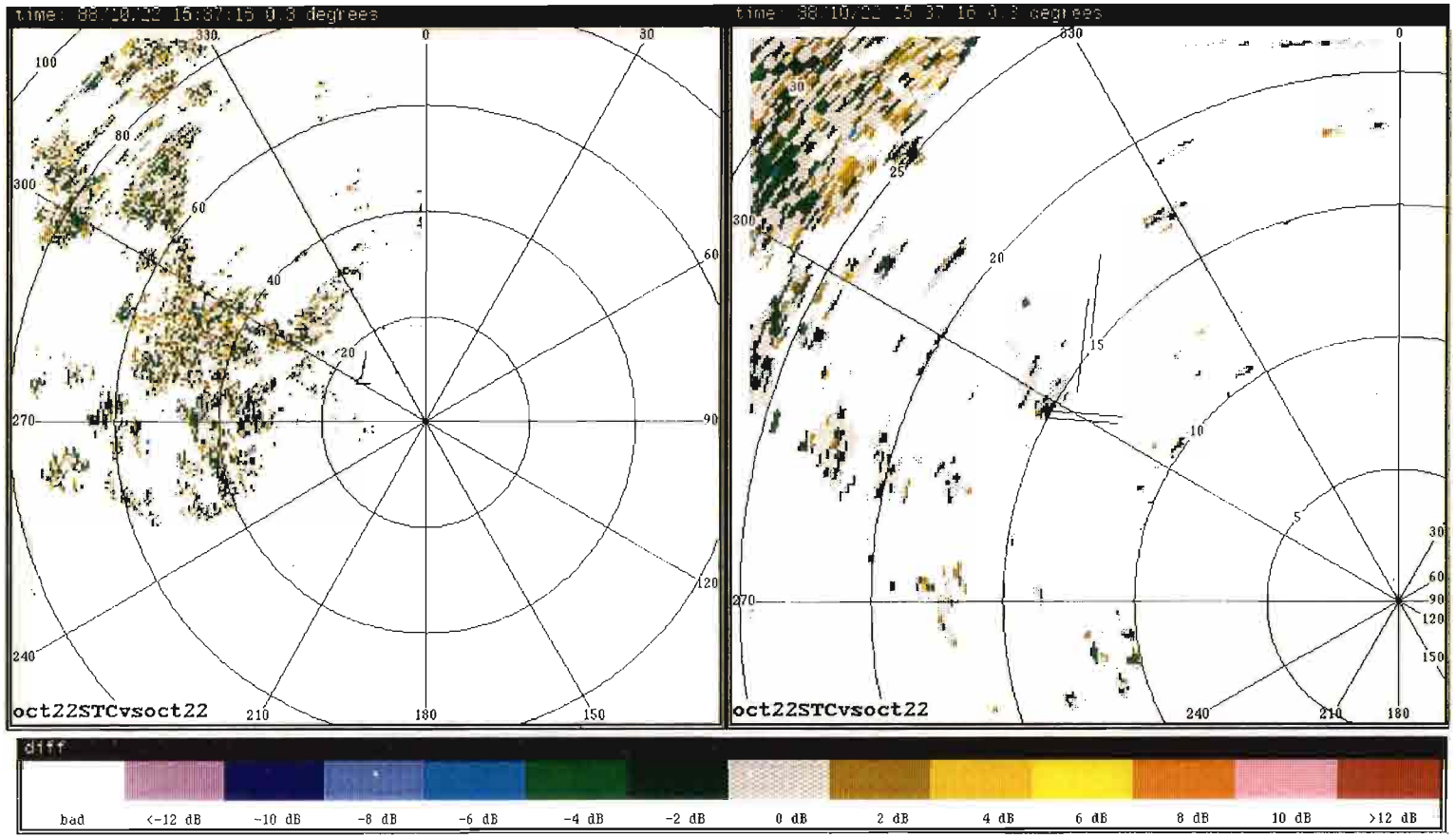

(a) (b)

Fig 12. Difference map of baseline case showing clutter difference over 2.5 minutes. October 22, 15:34:51 UT (STC on) minus October 22, 15:37:16 UT (STC off). First 10 km not displayed. (a) Full range view, (b) Enlarged view of Stapleton airport area.

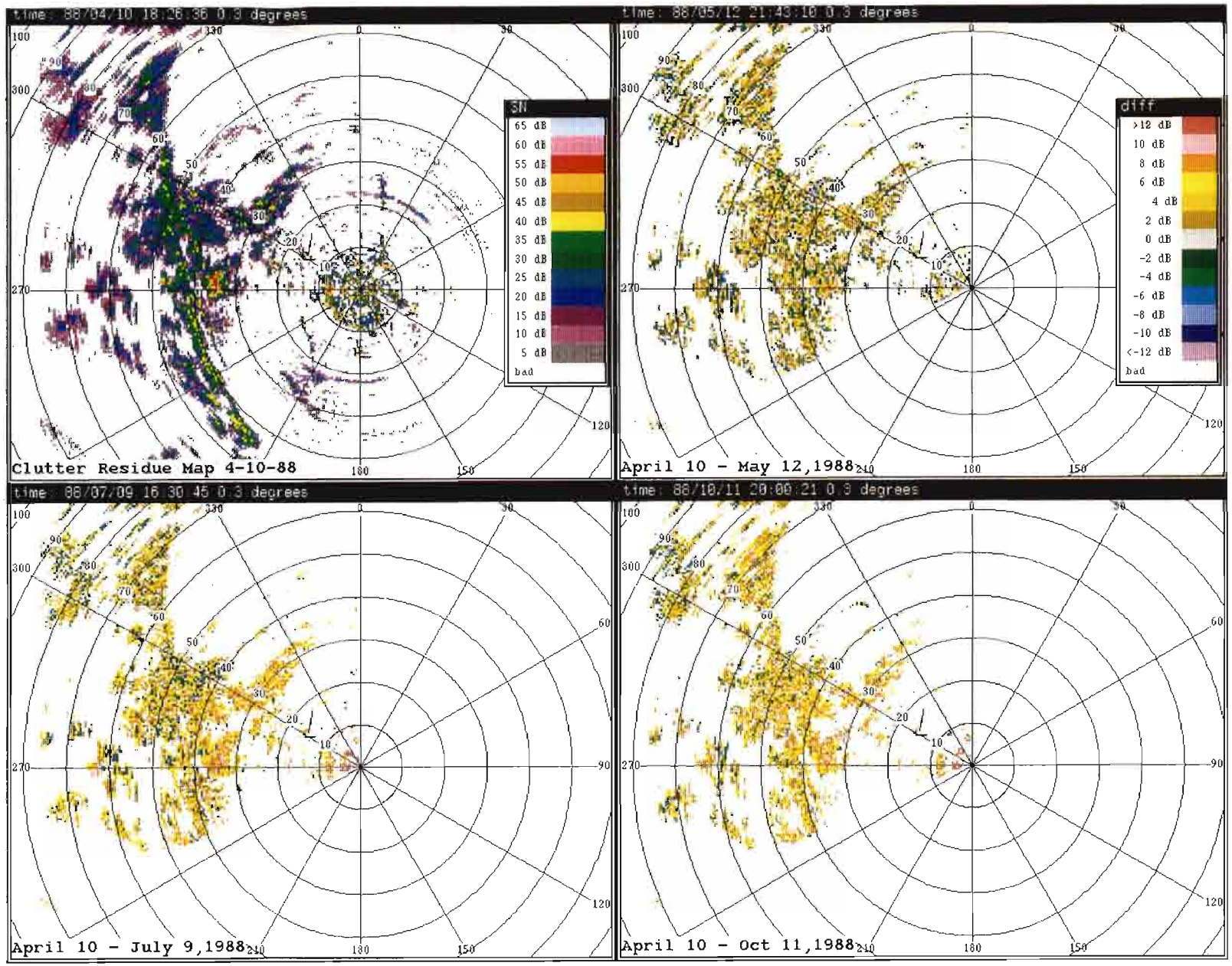

(a) (b) (c) (d)

Fig 13. Clutter residue map for April 10, 1988 and difference maps relative to April 10, 1988. (a) Clutter residue map for April 10, 1988 (reference), (b) April 10 minus May 12, (c) April 10 minus July 9, (d) April 10 minus October 11, (e) Enlarged view of (a), (f) Enlarged view of (b), (g) Enlarged view of (c), (h) Enlarged view of (d).

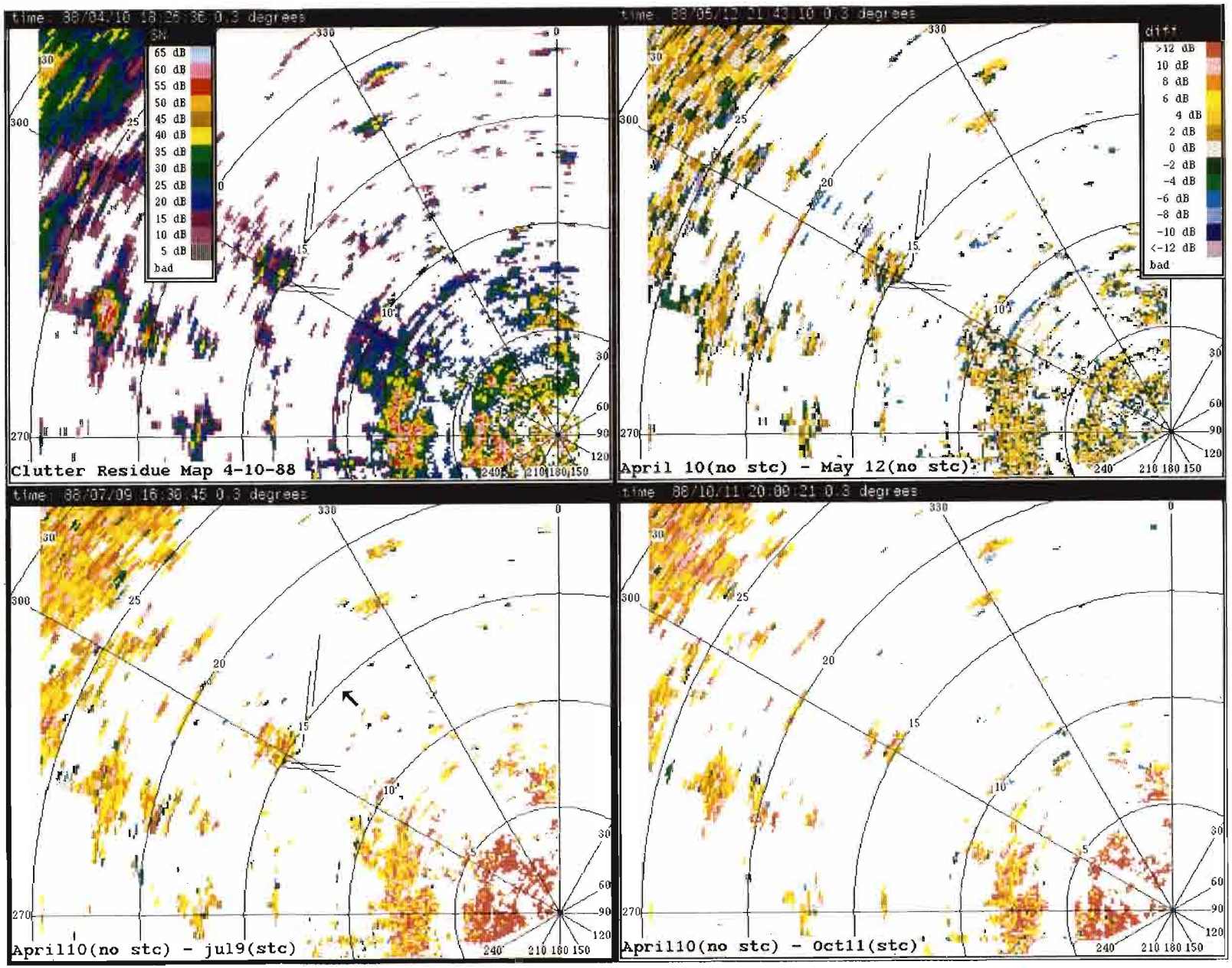

Fig 13. (continued) Clutter residue map for April 10, 1988 and difference maps relative to April 10, 1988. (a) Clutter residue map for April 10, 1988 (reference), (b) April 10 minus May 12, (c) April 10 minus July 9, (d) April 10 minus October 11, (e) Enlarged view of (a), (f) Enlarged view of (b), (g) Enlarged view of (c), (h) Enlarged view of (d).

Some general observations can be made regarding these clutter differences:

a. On average, the mean clutter is reduced over the April to October period. This is indicated by the positive values in the mean of the difference statistics, and the general preponderance of yellow-shifted tones in the maps (the difference is taken by subtracting the second map from the first).

b. The spatial changes are mostly uniform; that is, generally there do not appear to be any significant localized changes or spatial inhomogeneities, but rather the entire clutter residue field (except for some isolated cells) changes more or less together.*

c. Along with the change in the mean, the overall statistics indicate that a standard deviation, σ, of about 4 dB is typical for all cases except for the anomalous April 10-minus-August 24 case (6.2 dB). Inasmuch as the remaining difference maps indicate a σ of about 4 dB and are roughly similar visually, one can conclude tentatively that a 4 dB σ represents an acceptable difference between maps, and that a σ of about 6 dB suggests that map updates are needed. A σ of about 4 dB appears to be representative of the difference statistics to be expected between two residue maps.**

The following observations are made relative to the individual difference maps:

a. Figure 13(b), April 10 minus May 12. This particular comparison shows a very small mean difference and fairly uniformly-distributed positive and negative fluctuations over the entire map, indicating a great deal of similarity between the

---

* An exception is the April 10-minus-August 24 map, which is not shown here but will be discussed in the next section. This particular map exhibits unusual clutter characteristics, due most likely to an anomalous propagation (AP) condition.

** The results of a statistical study by Lee [8] indicate that about a 2 dB r.m.s. error can be expected in the median estimation for a single map based on a 20 sample data set.

maps on these two dates. The "speckled" appearance of this map, consisting primarily of random cell-to-cell fluctuations, points to very little substantive clutter change over this 32-day period. Peak cell-to-cell differences are on the order of 6 dB, slightly higher than the fluctuations noted in the baseline reference map. It is concluded from this comparison that the earlier map would adequately represent the clutter state at the later date if an updated replacement map were not available.

b. Figure 13(c), April 10 minus July 9. This difference map, representing an elapsed time of 90 days, shows somewhat less spatial uniformity than the previous map. A weaker clutter region in July is evident in approximately the 20-40 km range sector, with a more homogeneous clutter region in the mountains beyond (which contains more vegetation). There are also a number of individual cells that have differences in the 10-12 dB range. These changes suggest that the April 10 map was not appropriate for use by July 9. (The differences in the 0-10 km region, especially visible in the expanded map, Figure 13(g), represent primarily a difference in residue level associated with the use of STC).*

c. Figure 13(d), April 10 minus October 11. This map extends the comparison to a period of 184 days. Although it is unlikely that maps having this longevity would function properly, it is included here for the sake of completeness. Overall, this map shows a heavy bias toward a lower clutter level in October (more yellow tones), and contains many individual cell differences on the order of 10-12 dB. Roughly speaking, however, the clutter change has been more or less uniform without strongly defined spatial patches, and is in many respects a "normal looking" difference map but with a lower overall clutter intensity.

---

* Without STC, the receiver saturated on clutter cells within 10 km. In such cases, there is a high clutter residue level. With STC, the clutter returns fall in the linear range of the receivers and are suppressed to a greater extent by the clutter filters.

6.2.3 Shorter Term (Map-To-Map) Clutter Residue Changes

The previous section analyzed the evoluton of the clutter residue for progressively longer periods of time beginning in April and ending in October. This section considers the differences between successive maps; that is, from map to map over this time period. The time intervals between difference maps in this set range from 32 days to 58 days, with an additional comparison included for a 94-day interval that bypasses the AP contaminated data of August 24. These intervals are shown in the sequence of plates in Figure 14. Table 4 lists the maps, the time intervals covered, and the related map-difference statistics. The first map (April 10 minus May 12)

TABLE 4

MAP-MAP DIFFERENCES

Figure	Dates	Time Span	Difference Statistics	
			Mean	Std Dev
14a,e	Apr 10 - May 12	32 days	1.1	3.7
14b,f	May 12 - Jul 9	58	2.1	4.0
14c,g	Jul 9 - Aug 24 (anomalous)	46	-1.6	6.4
14d,h	Jul 09 - Oct 11	94	0.4	3.7

was shown in the preceding section but is repeated here for continuity.

The following observations can be made relative to these maps:

a. Figure 14(a), April 10 minus May 12. As noted earlier there is a great deal of

similarity between these two dates, indicating little change in clutter structure over the 32-day period.

b. Figure 14(b), May 12 minus July 9. Because of the similarity between the map pair above (which also includes the May 12 map), this comparison is similar to that observed in the preceding section for the April 10-minus-July 9 pair. That is, there is a somewhat weaker clutter region out to about 40 km where the Rocky Mountain foothills begin, followed by a more or less homogeneous region beyond. In addition, there are small groups of cell clusters that differ by up to 10-12 dB. These differences appear to be large enough to warrant an updated map.

c. Figure 14(c), July 9 minus August 24. The difference in clutter residue between these two dates shows a considerable spatial change. There is considerably more clutter in the region of the foothills and the lead edge of the mountain range on August 24. Beyond about 40 km, the situation reverses and the clutter becomes weaker. This unusual behavior is most likely due to anomalous propagation (AP) where refractive bending takes place. In support of this notion was the observation by the radar operators in real time that distant clutter was abnormally present. Furthermore, it was noted that other maps, generated from measurements made at about the same time, showed considerable differences in clutter structure. The clutter pattern on this difference map is also consistent with that observed for maps taken at slightly different elevation angles, which leads to the conclusion that refractive bending was taking place. For example, Figure 15(b) shows the difference between two maps generated for 0.3 deg and 0.2 deg elevation angles and recorded only a few minutes apart. Figure 15(a) repeats the July 9-minus-August 24 anomalous difference map for comparison. (Figures 15(c) and (d) are the corresponding maps with the airport area enlarged.) A similar pattern is evident here, where the lower antenna beam shows stronger clutter returns at near ranges, and the distant clutter

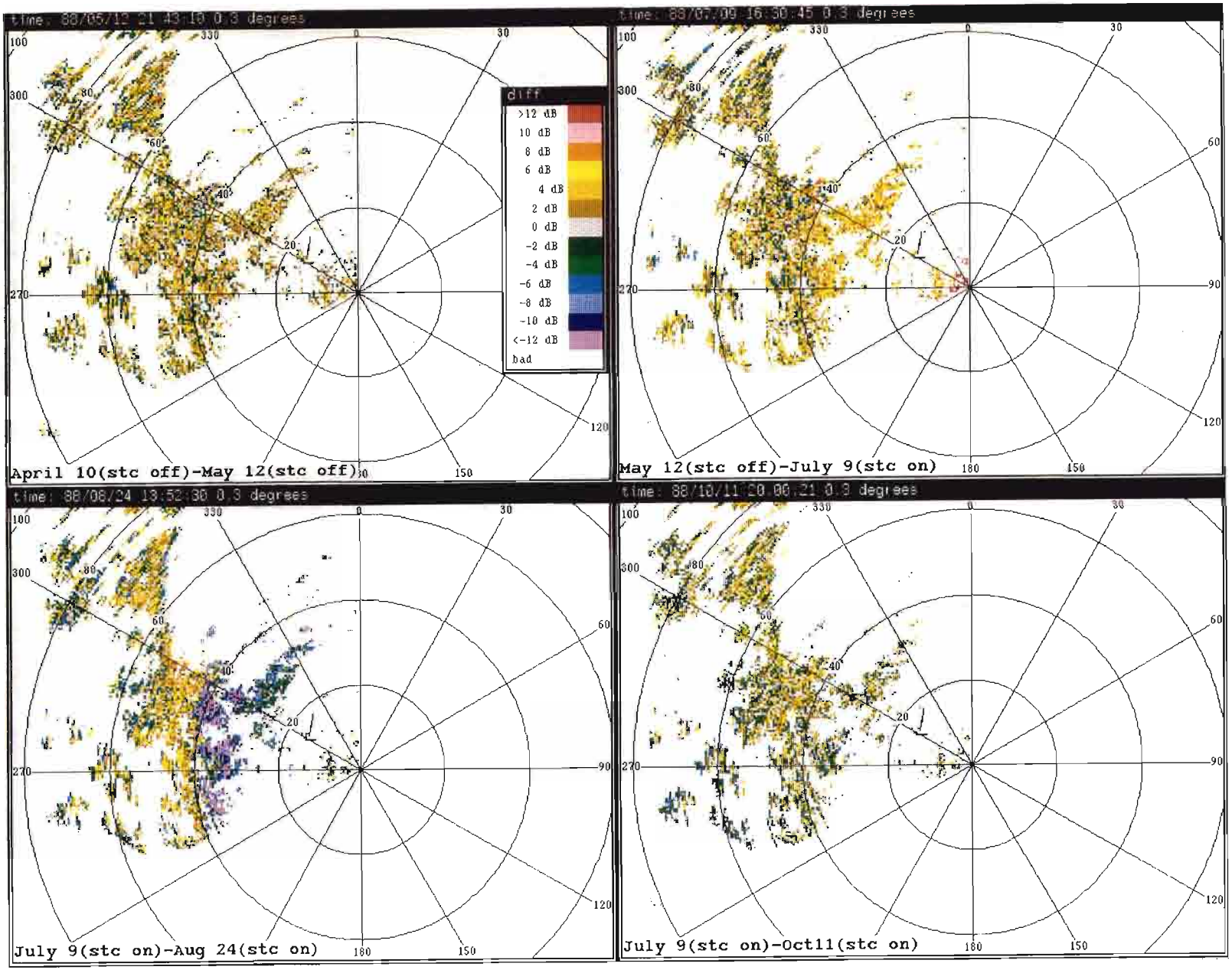

Fig 14. Difference maps based on map-to-map comparisons. (a) April 10 minus May 12, (b) May 12 minus July 9, (c) July 9 minus August 24 (anomalous propagation case), (d) July 9 minus October 11, (e) Enlarged view of (a), (f) Enlarged view of (b), (g) Enlarged view of (c), (h) Enlarged view of (d).

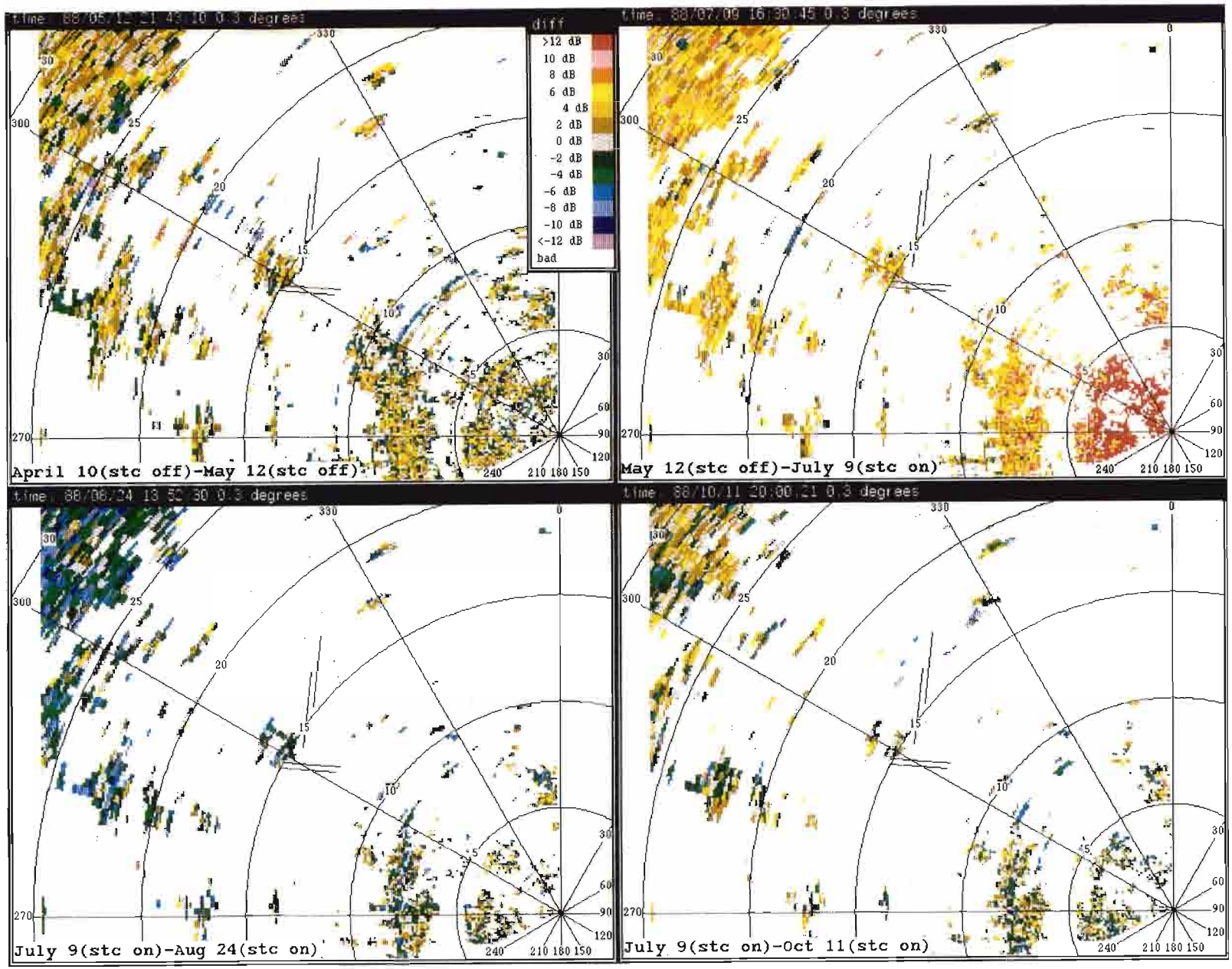

(e) (f) (g) (h)

Fig 14. (continued) Difference maps based on map-to-map comparisons, (a) April 10 minus May 12, (b) May 12 minus July 9, (c) July 9 minus August 24 (anomalous propagation case), (d) July 9 minus October 11, (e) Enlarged view of (a), (f) Enlarged view of (b), (g) Enlarged view of (c), (h) Enlarged view of (d).

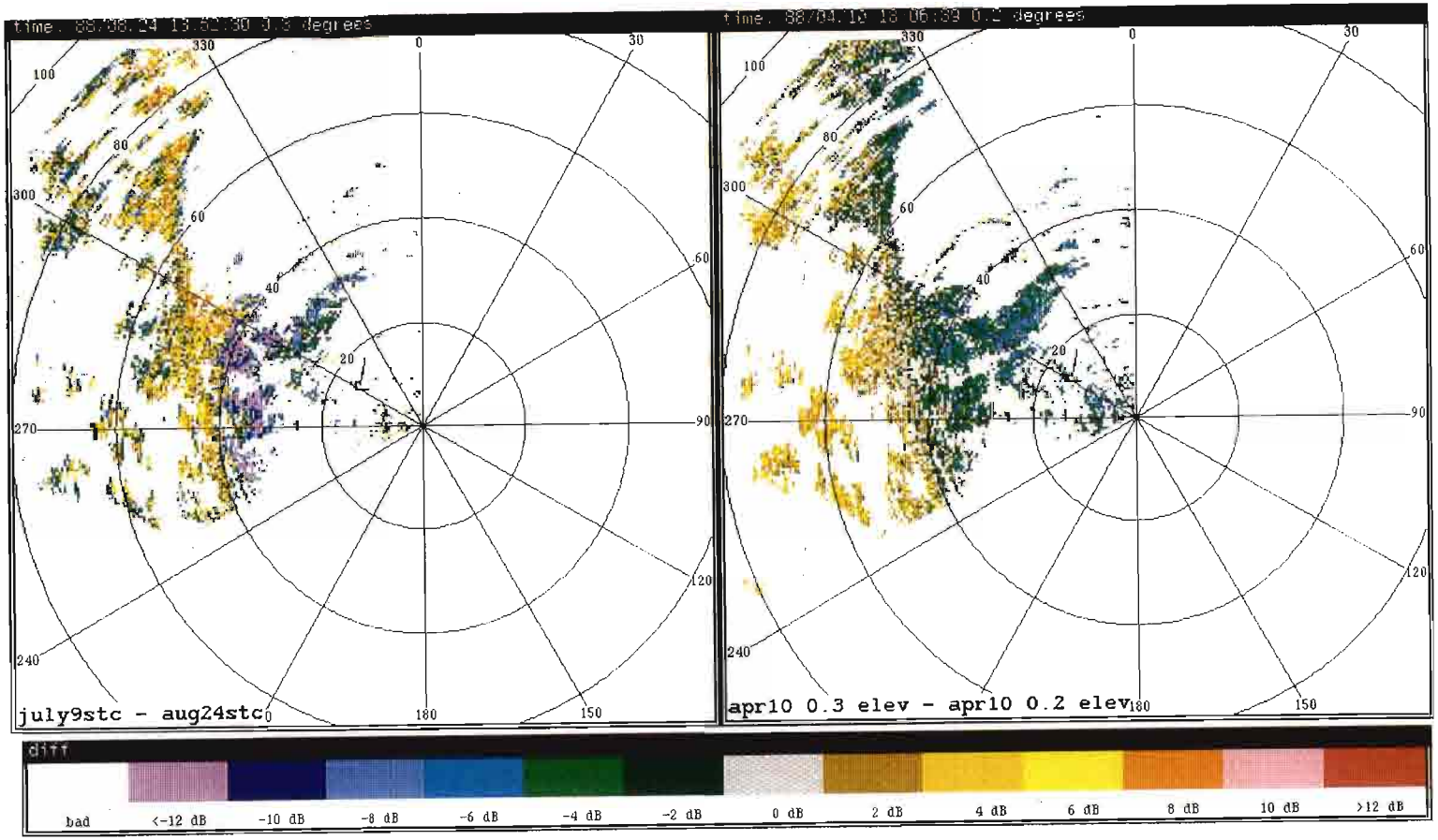

Fig 15. Example of likely anomalous propagation (AP) ducting condition. (a) July 9 minus August 24 difference map, (b) 0.3 deg minus 0.2 deg elevation difference map for April 10, (c) Enlarged view of (a), (d) Enlarged view of (b).

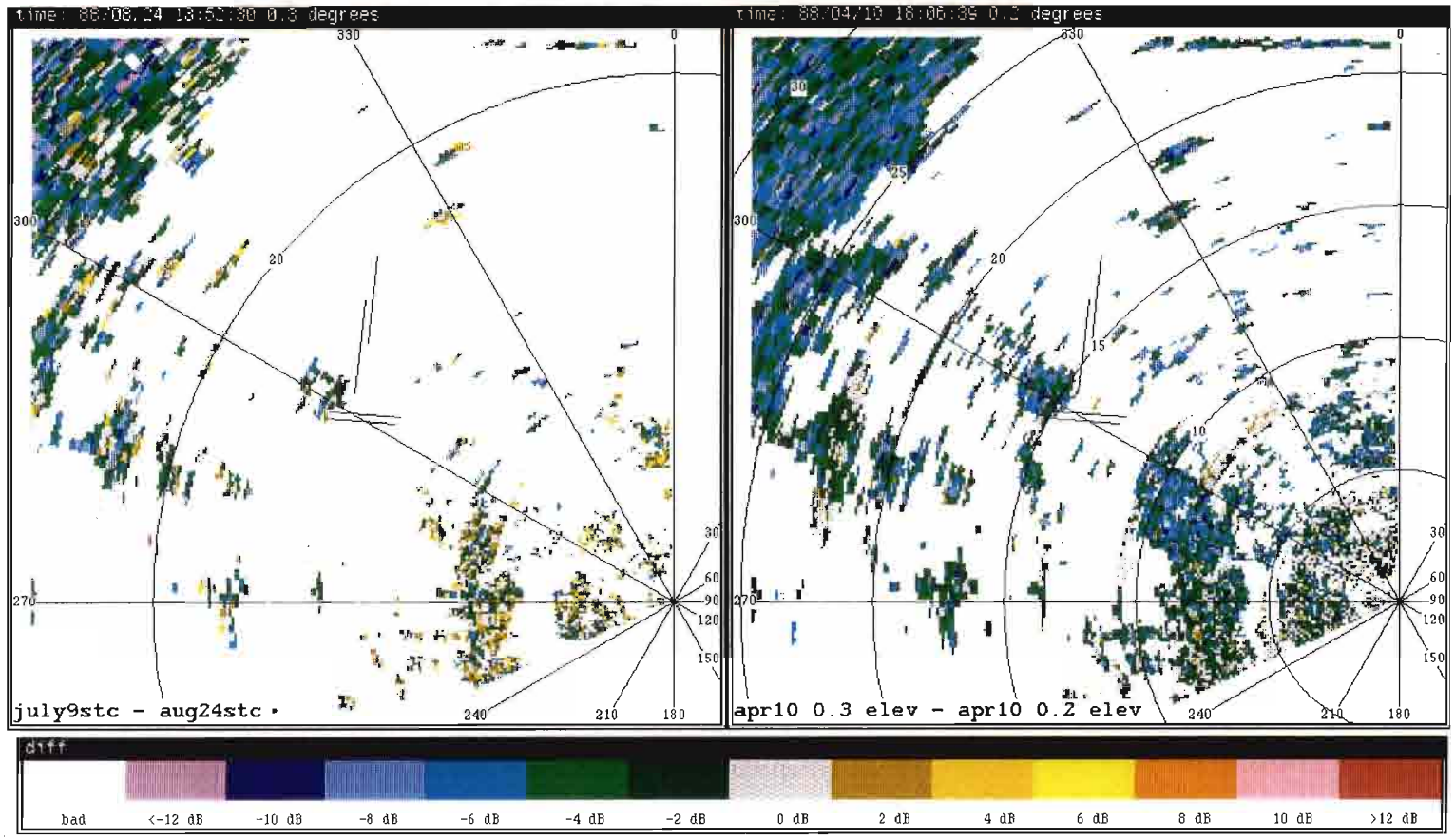

(c) (d)

Fig 15. (continued) Example of likely anomalous propagation (AP) ducting condition. (a) July 9 minus August 24 difference map, (b) 0.3 deg minus 0.2 deg elevation difference map for April 10, (c) Enlarged view of (a), (d) Enlarged view of (b).

is effectively shadowed in the mountain regions. A differential change in intensity of at least 12 dB has taken place over these ranges. These gross spatial changes make maps recorded under AP conditions unsuitable for editing of weather data recorded under normal propagation conditions. These differences also emphasize the need for

(1) development of procedures for recognizing when AP is present and editing the data appropriately in such cases, and

(2) determining when AP is present so that the operators do not attempt to make a "normal propagation condition" clutter residue map.

d. Figure 14(d), July 9 minus October 11. Since the above map comparison was affected by AP, and a study of the normal progression of clutter changes is not possible for the August 24 date, this difference map bypasses that date and shows the comparison with the next map (October 11). This 94-day interval shows a more normal map without the AP effects. Local differences are evident in the form of cell *clusters*, unlike the random cell-to-cell fluctuations of similar magnitude (about 4 dB peak) observed in the best map comparison so far: the 32-day, April 10-minus-May 12 map. On an overall statistical basis, the two maps are similar, but it is evident in the appearance of the latter map that the differences vary in terms of larger patches rather than in cell-to-cell fluctuations. Because of these differences, one would choose to update the map; however, it can be argued that the similarity is such that if one had no other choice, the July map would be usable in October. This comparison also lends weight to the conclusion that the August 24 map is anomalous, since this longer interval, encompassing as it does the August 24 date, shows a smoother change in clutter residue levels.

7.0 SUMMARY AND CONCLUSIONS

It is concluded that the clutter environment in Denver, as reflected in the clutter residue maps generated for the April-October 1988 time period, did not show a

marked change over long periods, and that on average, the clutter weakened as the season progressed. There was remarkable agreement between the maps of April 10 and May 12, representing an elapsed time of 32 days. Beyond this time, the map differences were enough to warrant an update, but could arguably be used if necessary for a longer period. The 94-day interval from July 9 to October 11, for example, showed surprising agreement despite some differences in the fine structure of the clutter.

Based on this experience, a map update at monthly to bimonthly intervals would be adequate in the Denver area. For planning purposes, however, maps generated on a monthly basis would be preferable, and the existing maps replaced as necessary. The more frequent updates would recognize the need to have fairly exact clutter estimates available for the automated wind shear detection algorithms, which are sensitive to the clutter field.

It would have been desirable to have had more frequent map samples to define a more quantitative measure of acceptable map differences. Nevertheless, on the basis of the maps presented here, it appears that an acceptable upper bound difference between maps of about 4 dB standard deviation and a 1 dB mean in overall statistics can be established. Larger differences than this would likely point to significant clutter changes; although moderate, fairly uniform changes in the mean can likely be adjusted by the Xcr parameter. Also, a necessary ingredient in map comparisons is the visual appearance of the maps. A speckled appearance is indicative of random fluctuations from cell to cell and is usually acceptable, whereas cluster-sized changes would likely indicate a true clutter change, even though the overall statistics might be similar. Without a precise metric measure to establish the point at which a map becomes invalid, a visual determination of map differences is necessary.

The presence of AP drastically distorts the clutter map and should obviously be avoided during clutter measurements intended for normal propagation editing. This requirement accompanies the need to ensure that clutter measurements are always performed on clear, weather-free days. Weather data recorded on days when AP is present are subject to large clutter editing errors and should be used with caution. Since AP can occur during hazardous weather measurements (a very strong microburst was observed by accident when making AP measurements during 1986 in Huntsville), a procedure needs to be developed for clutter residue editing when AP is present.

The intensity and structure of the clutter is quite sensitive to the elevation angle at which the measurements are made, especially at the lower elevation angles considered here. A 0.1-deg elevation difference produces significant clutter change, particularly at a location like the Denver site where the terrain slopes down from the radar, and the flat lands run to the mountains in the distance. A small change in elevation angle is accompanied by a large increase in close range clutter because of added ground illumination, followed by shadowing at longer distances. A differential change in clutter intensity of at least 12 dB was noted between the closer ranges and the mountain region in the 0.3 deg-minus-0.2 deg elevation maps shown. This sensitivity to elevation angle points to the need for maintaining uniform elevation scans during clutter measurements, as well as precise elevation angle repeatability, so that weather data scans, conducted at different times, do not deviate from the elevation angle at which the maps were recorded.

The results reported here apply to the Denver location only. Other sites will have their own unique characteristics. Additional studies need to be conducted at other

sites where the characteristics differ significantly, particularly those where more vegetation variation can be expected such as in heavily forested areas.

APPENDIX A

TDWR TESTBED RADAR CHARACTERISTICS

ANTENNA	
Type	Paraboloid
Aperture	28 ft.
Gain	46.25 dB
Sidelobe ratio	<-25 dB
Beamwidth	1.0 deg one way
Polarization	Horizontal
Max rotation rate	30 deg/s
TRANSMITTER	
Source	Klystron
Frequency	2865 Mhz (Denver)
Wavelength	10.48 cm
Peak power	1.1 MW
Pulse width	0.65 microsecond
PRF	700-1220 pps, and 350-610 pps (half-PRF mode)
RECEIVER	
Noise Figure	-7.5 dB
Bandwidth	1.3 Mhz
STC	Pin diode at RF
STC curve	$1/R^2$, 0 to 10 km (PROM)
Min. detectable signal	-107 dBm
Sensitivity at 50 Km	-4.6 dBz (0 dB SNR)
AGC	"instantaneous" (max 48dB)
SIGNAL PROCESSOR	
A/D Converters	11 bits + sign I, 11 bits + sign Q, plus 4 bits AGC
Effective internal Dynamic Range	90 dB
Clutter filter suppression	50 dB on stationary tower
Number of range gates	800
Range gate spacing	120 meters
Algorithm	Pulse-pair processing
Processor output	0, 1, 2 spectral moments or I, Q time series

ACKNOWLEDGEMENT

The work described here represents the efforts of many members of Group 43. Special mention should go to E. Ducot who directed the map software development process, S. Troxel for his contributions to the development and understanding of the map programs, P. Biron who put in a great effort in generating the maps, S. Stanfill who programmed the median processing software, B. Stevens who painstakingly implemented the clutter editing features in the real time program, Denver site personnel: M. Isaminger, N. Fischer, and C. Curtiss who not only contributed the clutter measurements but provided invaluable assessments of clutter map performance, and group members who offered their expertise during the study and the writing of this report.

REFERENCES

1. D.R. Mann, "TDWR Clutter Residue Map Generation and Usage," MIT Lincoln Laboratory Project Report ATC-148 (29 January 1988).

2. J.E. Evans, "Ground Clutter Cancellation for the NEXRAD System," MIT Lincoln Laboratory Project Report ATC-122 (19 October 1983).

3. S.C. Crocker, "TDWR PRF Selection Criteria," MIT Lincoln Laboratory Project Report ATC-147 (15 March 1988).

4 S.D. Campbell and M.W. Merritt, "Advanced Microburst Recognition Algorithm," MIT Lincoln Laboratory Project Report ATC-145 (in preparation).

5. D. Klingle-Wilson et al., "Gust Front Detection for the Terminal Doppler Weather Radar: Part 2, Performance Assessment," submitted to Third International Conference on the Aviation Weather System (January 1989).

6. R.E Rinehart, internal document (11 August 1987).

7. M.E. Weber, "Ground Clutter Processing for Wind Measurements with Airport Surveillance Radars," MIT Lincoln Laboratory Project Report ATC-143 (4 November 1987).

8. T. Sen Lee, MIT Lincoln Laboratory, private communication.